AN APPROXIMATE FAST FOURIER TRANSFORM TECHNIQUE FOR VERNIER SPECTRAL ANALYSIS

Albert H. Nuttall

Naval Underwater Systems Center

Prepared for:

Naval Ship Systems Command

16 August 1974

UNCLASSIFIED

SECURITY CLASSIFICATION OF THIS PAGE (When Data Entered)

REPORT DOCUMENTATION PAGE		READ INSTRUCTIONS BEFORE COMPLETING FORM
1. REPORT NUMBER TR 4767	2. GOVT ACCESSION NO.	3. RECIPIENT'S CATALOG NUMBER AD 785850
4. TITLE (and Subtitle) AN APPROXIMATE FAST FOURIER TRANSFORM TECHNIQUE FOR VERNIER SPECTRAL ANALYSIS		5. TYPE OF REPORT & PERIOD COVERED 6. PERFORMING ORG. REPORT NUMBER
7. AUTHOR(s) Albert H. Nuttall		8. CONTRACT OR GRANT NUMBER(s)
9. PERFORMING ORGANIZATION NAME AND ADDRESS Naval Underwater Systems Center New London Laboratory New London, Connecticut 06320		10. PROGRAM ELEMENT, PROJECT, TASK AREA & WORK UNIT NUMBERS A-758-02 SF 11 121 701
11. CONTROLLING OFFICE NAME AND ADDRESS Naval Ships Systems Command (PMS-302-4) Washington, D. C. 20360		12. REPORT DATE 16 August 1974 13. NUMBER OF PAGES 52
14. MONITORING AGENCY NAME & ADDRESS(if different from Controlling Office)		15. SECURITY CLASS. (of this report) UNCLASSIFIED 15a. DECLASSIFICATION/DOWNGRADING SCHEDULE
16. DISTRIBUTION STATEMENT (of this Report)		
17. DISTRIBUTION STATEMENT (of the abstract entered in Block 20, if different from Report)		
18. SUPPLEMENTARY NOTES		
19. KEY WORDS (Continue on reverse side if necessary and identify by block number) Vernier Spectral Analysis Approximate Spectral Analysis Fast Fourier Transform Overlapped Time Weighting Delay Weighting Dolph-Chebyshev Weighting		

20. ABSTRACT (Continue on reverse side if necessary and identify by block number)

An approximate and quick fast Fourier transform technique for vernier spectral analysis is derived and tested for several candidate time- and delay-weightings, and for overlaps of the time weightings. For 50 percent overlap, the use of a simple cosine lobe for the time weighting yields spurious spectral sidelobes at least 23 dB below the main peak, whereas Dolph-Chebyshev time weighting achieves -33 dB sidelobes. For 75 percent overlap, use of a (cosine)^5 lobe for the time weighting

DD FORM 1 JAN 73 1473 EDITION OF 1 NOV 66 IS OBSOLETE
S/N 0102-014-6601

UNCLASSIFIED

SECURITY CLASSIFICATION OF THIS PAGE (When Data Entered)

20. Cont'd.

yields sidelobes at least 54 dB down, whereas Dolph-Chebyshev time weighting achieves -86 dB sidelobes. In both cases of overlap, use of delay weighting is also required and is taken as a Hanning weighting. Extensions to other overlaps and weightings are possible from the fundamental relations presented and from the sample program furnished.

PREFACE

This report was prepared under NUSC Project No. A-758-02, "Computer-Aided Detection, Localization, and Classification (CADLAC)," Principal Investigator, H. S. Newman (Code TD111) and Navy Subproject and Task No. SF11 121701, Program Manager, D. Porter (Code PMS-302-4). This work was also supported by NUSC Project No. A-752-05, "Applications of Statistical Communication Theory to Acoustic Signal Processing," Principal Investigator, A. H. Nuttall (Code TC) and Navy Subproject and Task No. ZF61 112 001, Program Manager, Dr. J. H. Huth (CNM Code MAT-03L4).

The Technical Reviewer for this report was H. S. Newman (Code TD111).

A preliminary version of the technique investigated here was suggested by Mr. H. S. Newman and Dr. N. L. Owsley. The author would like to acknowledge many helpful suggestions and discussions held with these gentlemen.

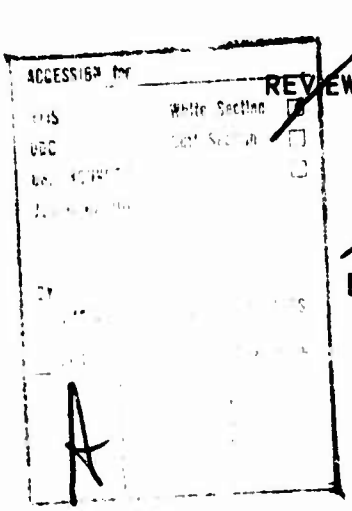

REVIEWED AND APPROVED: 16 August 1974

W. A. Von Winkle
Director, Science & Technology

The author of this report is located at the New London Laboratory, Naval Underwater Systems Center, New London, Connecticut 06320.

TABLE OF CONTENTS

LIST OF TABLES

LIST OF ILLUSTRATIONS

LIST OF SYMBOLS

t	time
$x(t)$	data waveform
Δ	sampling increment in time
f	frequency; analysis frequency
$V(f)$	voltage density spectrum
$u(t)$, $w(t)$	temporal weighting
$\delta_\Delta(t)$	impulse train, equation (2)
$X(f)$	voltage density spectrum of $x(t)$
$U(f)$, $W(f)$	temporal window
L	number of samples in duration of temporal weighting $u(t)$
τ	delay
$a(f,\tau)$	spectral-delay function
ν	vernier frequency
$d(\tau)$	delay weighting
$Y(f,\nu)$	vernier spectrum
L_w, L_d	length of temporal weighting, delay weighting
S	separation of delays
M	number of delay increments
N	number of samples in duration of temporal weighting $w(t)$
I_S	integer number of sampling increments in delay S
$D(\nu)$	delay window
f_o	excitation frequency of pure tone

REVERSE BLANK

AN APPROXIMATE FAST FOURIER TRANSFORM TECHNIQUE FOR VERNIER SPECTRAL ANALYSIS

INTRODUCTION

To detect the presence of very narrowband weak signals in noise, and to measure their center frequencies accurately, it is necessary to Fourier transform a long time segment of the available process. When the center frequencies of the signal components are unknown and the total search bandwidth of interest is large, this procedure demands storage and computation of many degrees of freedom, that is, search of a large time-bandwidth product space. It would be advantageous if a quick, coarse search for narrowband components could be conducted, followed by a finer vernier analysis over a limited band where the presence of narrowband components has been indicated. Such an adaptive procedure would be less time-consuming and require less storage. Also, if the procedure did not need to be exact, but yielded an approximation with acceptable sidelobes, the required storage and computation might be reduced further.

This report presents just such a technique, which

1. accepts the input process in smaller time segments as they are available,

2. performs a reasonable-size weighted fast Fourier transform (FFT) on each overlapped segment,

3. stores only that frequency portion (at each segment) where narrowband components are indicated to be present, and

4. performs a small-size weighted FFT over the total data record available, for each frequency bin stored.

Steps 1 and 2 permit smaller-size FFTs than would be required if the total data record were spectrally analyzed in one operation. Steps 3 and 4 constitute the adaptive feature of this technique. The last transform over time (delay) in step 4, for each frequency bin, is a vernier frequency analysis, measured from the center of each bin; the degree of approximation of this technique is the subject of this report.

Some past work on performing large-size FFTs by means of several smaller FFTs is reported in references 1 and 2. The methods reported there are exact, but they consume more time and require more storage than the method to be presented here. In particular, the two methods of reference 1 require too many small-size FFTs, and the method of reference 2 requires additional multiplications by complex exponentials and a fair amount of storage. The approximate technique of reference 3 is similar to the one outlined above, up to step 4, with the notable exception of overlapped weighting; at that point the technique of reference 3 requires transformation back to the time domain followed by another transform to the desired frequency domain. Additional transforms are required in this last technique, and it produces greater sidelobes than the new technique, especially when the temporal weighting is judiciously selected.

FUNDAMENTAL SPECTRAL RELATIONSHIPS

LARGE-SIZE FFT APPROACH

Before embarking on the approximate technique, we review the standard large-size FFT approach to spectral analysis. Suppose a data waveform $x(t)$ is sampled at time instants $n\Delta$, n integer. Then the voltage density spectrum that can be computed is*

$$\begin{aligned} V(f) &\equiv \int dt \exp(-i2\pi ft)\ x(t)\ u(t)\ \Delta\ \delta_{\Delta}(t) \\ &= \Delta \sum_{n} \exp(-i2\pi fn\Delta)\ x(n\Delta)\ u(n\Delta)\ , \end{aligned} \tag{1}$$

where $u(t)$ is a temporal weighting deliberately imposed to control spectral sidelobes, as will be discussed shortly; see figure 1A. The finite duration of $u(t)$ terminates the integral and sum in equation (1) at finite limits. The impulse-train function in (1) is defined as the infinite sum

$$\delta_{\Delta}(t) \equiv \sum_{n} \delta(t - n\Delta)\ . \tag{2}$$

The integral representation in (1) allows us to express†

$$V(f) = X(f) \bullet U(f) \bullet \delta_{1/\Delta}(f)\ , \tag{3}$$

*All integrals are over the range of nonzero integrand.

†The Fourier transform of the lower-case time function $x(t)$ is the upper-case frequency function $X(f)$; this notation is used throughout.

where ● denotes convolution, and, in keeping with (2),

$$\delta_{1/\Delta}(f) = \sum_m \delta\left(f - \frac{m}{\Delta}\right) . \qquad (4)$$

Thus, the observed spectrum V(f) is the convolution of X(f) with the set of windows* $U(f) \bullet \delta_{1/\Delta}(f)$, which is depicted in figure 1B.

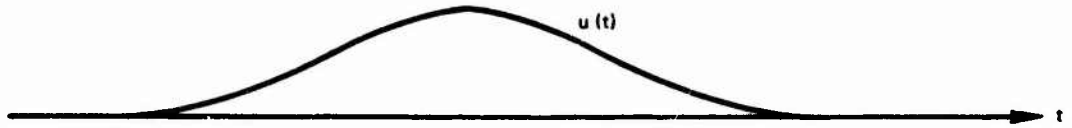

Figure 1A. Temporal Weighting

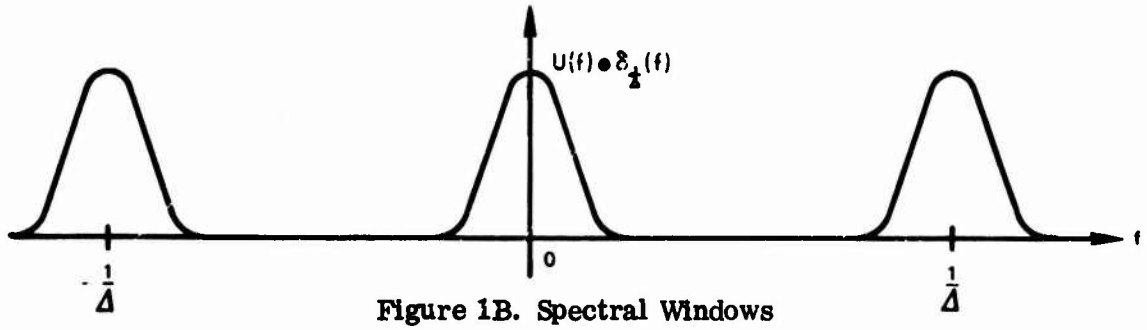

Figure 1B. Spectral Windows

Figure 1. Time and Frequency Relationships

Because the ideal spectral window is a single impulse at f = 0, the aliased mainlobes at m/Δ, $m \neq 0$, are undesired. Also, the window U(f) is desired to be narrow, with very small sidelobes. Since the weighting u(t) is of limited duration, the mainlobe width of U(f) is not zero, but is inversely proportional to the time duration.

Now, if the voltage density spectrum V(f) is computed at multiples of $(L\Delta)^{-1}$, where $L\Delta$ is the time duration of u(t), we obtain

$$V\left(\frac{p}{L\Delta}\right) = \Delta \sum_n \exp(-i2\pi np/L)\, x(n\Delta)\, u(n\Delta) , \quad p \text{ integer} . \qquad (5)$$

*In the time domain, u(t) is called a weighting; the corresponding Fourier transform in the frequency domain, U(f), is called a window. This nomenclature is used throughout.

Since V(f) is periodic of period $1/\Delta$ (see (1)), (5) need be computed at L different points; thus it can be realized as an L-point FFT of sequence $\{x(n\Delta)\ u(n\Delta)\}$. For fine frequency analysis (that is, large $L\Delta$) the size L of the FFT may be too large to compute easily, under storage and time limitations. The values in (5) are samples of the convolution of figure 1B with voltage density spectrum X(f).

APPROXIMATE FFT TECHNIQUE

Just as we started above with an integral definition of a spectrum, then showed that samples of this spectrum were attainable with an FFT, we begin with the spectral-delay function, a, defined as

$$\begin{aligned} a(f,\tau) &\equiv \int dt \exp(-i2\pi ft)\, x(t)\, w(t-\tau)\, \Delta\delta_{\Delta}(t) \\ &= \Delta \sum_{n} \exp(-i2\pi fn\Delta)\, x(n\Delta)\, w(n\Delta - \tau)\ . \end{aligned} \tag{6}$$

The temporal weighting w is now delayed by τ seconds; if the duration of w is L_w seconds, the function $w(t-\tau)$ picks out a delayed portion of data x of length L_w, and subjects it to the same transform as in (1). This operation is depicted in figure 2A, where the temporal weighting can be located at aa, bb, ..., cc. This figure is drawn for 50 percent overlap of the temporal weightings; however, other overlaps are possible and recommended in some cases.

The next step, consistent with step 4 in the Introduction, is to perform a Fourier transformation on the delay variable τ, while holding frequency variable f fixed. The general definition is the vernier spectrum

$$\begin{aligned} Y(f,\nu) &\equiv \int d\tau \exp(-i2\pi\nu\tau)\, a(f,\tau)\, d(\tau)\, S\delta_{S}(\tau) \\ &= S \sum_{k} \exp(-i2\pi\nu kS)\, a(f,kS)\, d(kS)\ , \end{aligned} \tag{7}$$

where ν is the vernier frequency, $d(\tau)$ is called the delay weighting, and S is the separation increment in delay τ at which $a(f,\tau)$ must be computed; that is, S is the shift between temporal weighting locations (see figure 2A). Since the separation S in delays can be taken to be smaller than the temporal weighting duration L_w, (7) allows for overlapped weighted transformation of the available data (see (6)).

The operation described by (7) is depicted in figure 2B. When the Fourier transform (6) on weighted time segment aa is completed, the set of frequency components denoted by the vertical line of Xs at the end of segment aa are available. Similarly, frequency component values at the ends of segments bb, . . . , cc are indicated in figure 2B; these components correspond to delayed locations of the temporal weighting w. Now, for a fixed frequency, say f_1, the array of (delayed) frequency components indicated in a horizontal box in figure 2B is subjected to a delay weighting and is Fourier transformed according to (7), thereby yielding vernier spectrum $Y(f_1, \nu)$. Similar outputs are available for other (adjacent) frequencies of interest, such as f_2 or f_3 .

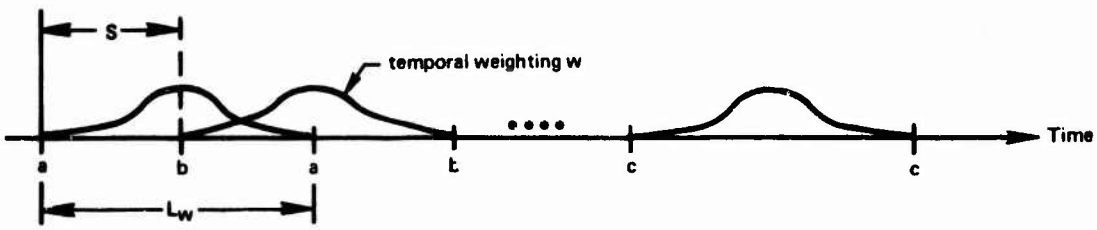

Figure 2A. Overlapped Temporal Weightings

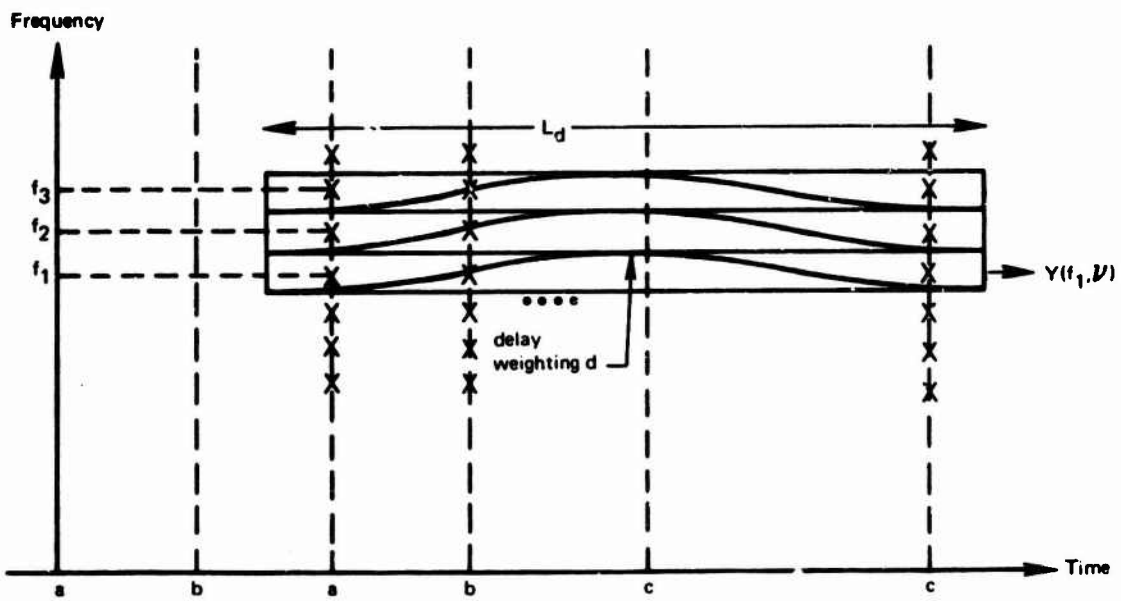

Figure 2B. Adjacent Delay Weightings

Figure 2. Temporal and Delay Weightings

Samples of the vernier spectrum in ν at multiples of $(MS)^{-1}$, where MS is the duration of delay weighting $d(\tau)$, are given by

$$Y\left(f, \frac{m}{MS}\right) = S \sum_k \exp(-i2\pi mk/M)\, a(f, kS)\, d(kS), \quad m \text{ integer}, \tag{8}$$

which can be realized as an M-point FFT of the sequence $\{a(f, kS)\, d(kS)\}$ of length M. The periodicity of $Y(f, \nu)$ in ν, of period $1/S$ (see (7)), means that (8) need be computed only at M different values of m.

Finally, samples of vernier spectrum Y in frequency f at multiples of $(N\Delta)^{-1}$ are given by (using (8))

$$Y\left(\frac{p}{N\Delta}, \frac{m}{MS}\right) = S \sum_{k=0}^{M-1} \exp(-i2\pi mk/M)\, a\left(\frac{p}{N\Delta}, kS\right) d(kS), \tag{9}$$

$$p = 0, 1, \ldots, N-1; \quad m = 0, 1, \ldots, M-1,$$

where delay weighting $d(\tau)$ has been selected so that samples $\{d(kS)\}$ are nonzero only for $k = 0, 1, \ldots, M-1$. The values of a needed in (9) are (using (6)) given by

$$a\left(\frac{p}{N\Delta}, kS\right) = \Delta \sum_n \exp(-i2\pi pn/N)\, x(n\Delta)\, w(n\Delta - kS). \tag{10}$$

In order to put (10) directly in the form of a standard FFT, we assume that the delay separation S is taken as an integer multiple of the sampling increment Δ:

$$S = I_s \Delta. \tag{11}$$

Then, if temporal weighting w has nonzero samples $\{w(n\Delta)\}$ only for $0 \le n \le N-1$, (10) becomes

$$a\left(\frac{p}{N\Delta}, kS\right) = \exp(-i2\pi pkI_s/N)\, \Delta \sum_{m=0}^{N-1} \exp(-i2\pi pm/N)\, x(m\Delta + kI_s\Delta)\, w(m\Delta), \tag{12}$$

$$0 \le p \le N-1, \quad 0 \le k \le M-1.$$

The exponential phase factor preceding the sum (FFT) in (12) takes on particularly simple forms for two special cases of delay separation S: For $I_S = N/2$, delay S is equal to half the temporal weighting duration L_W and is termed 50 percent overlap; for $I_S = N/4$, delay S is one-quarter of L_W and is termed 75 percent overlap. For these two cases,

$$\text{50 percent overlap, } I_S = N/2, \text{ phase factor} = (-1)^{pk} ; \qquad (13A)$$

$$\text{75 percent overlap, } I_S = N/4, \text{ phase factor} = (-i)^{pk} . \qquad (13B)$$

By proper branching in a computer program, no storage or complex multiplications are necessary to incorporate these phase factors in (12), prior to its usage in (9). (An alternative approach that completely circumvents the phase factor in (12) is described in appendix A.)

Equations (12) and (9) are the essential results of interest. We now interpret them by means of simple examples that will enable us to make good choices of temporal weighting w, delay weighting d, and separation (overlap) S.

INTERPRETATION OF THE VERNIER SPECTRUM

In appendix B, the vernier spectrum is shown to be given in terms of X by

$$Y(f, \nu) = \left[W(-\nu) \sum_m X\left(f + \nu - \frac{m}{\Delta}\right) \right] \bullet D(\nu) \bullet \delta_{1/S}(\nu) , \qquad (14)$$

where all the convolutions are on ν, with f held fixed. $D(\nu)$ is the delay window corresponding to the delay weighting $d(\tau)$.

The linearity of the two Fourier transforms, (6) and (7), on the data x(t) indicates that we can investigate the behavior for data components separately and merely add the results. The fundamental component is

$$x(t) = \exp(i2\pi f_o t), \quad X(f) = \delta(f - f_o) . \qquad (15)$$

At this point, we shall make a series of reasonable assumptions and requirements, and deduce desirable properties about the weightings and separations. The first assumptions are

(a) excitation frequency $f_o < (2\Delta)^{-1}$,

(b) coarse analysis frequency $f < (2\Delta)^{-1}$,

(c) $L_W >> \Delta$.

Assumption (a) avoids aliasing, (b) restricts analysis to the fundamental range, and (c) requires the temporal weighting to cover many samples of the process x(t). Furthermore, if

(d) temporal window W has low sidelobes,

the only term in the sum in (14), after substituting (15), that has substantial value is that for $m = 0$, and it yields

$$Y(f, \nu) \cong \left[W(f - f_0)\, D(\nu + f - f_0)\right] \circledast \delta_{1/S}(\nu) \quad . \tag{16}$$

A plot of this equation versus vernier frequency ν is given in figure 3, where L_d is the length (duration) of delay weighting $d(\tau)$. The narrow lobe at $\nu = f_0 - f$ is the desired component; this component is displaced from the coarse analysis frequency f (corresponding to $\nu = 0$) by $f_0 - f$ Hz, which places it at absolute frequency $f + (f_0 - f) = f_0$, as desired. The shape of this lobe is governed by the delay window D; thus, if

(e) $L_d \gg S$,

(f) delay window D has low sidelobes,

the large lobes separated by 1/S Hz in figure 3 will not overlap significantly, and potentially good spectral estimation is possible. The necessity of delay weighting is made obvious by these observations.

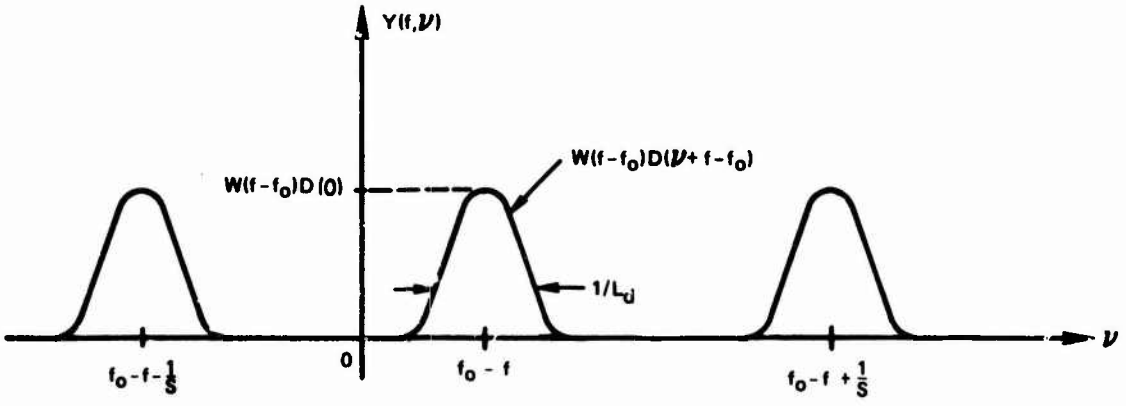

Figure 3. Vernier Spectrum

There are a few additional points worth noting about figure 3. The peak height of the lobes, $W(f - f_0)\, D(0)$, is a function of the exact location of the excitation frequency f_0 and the coarse analysis frequency f. This undesirable picket-fence effect* (which was not present in figure 1) can be minimized:

(g) choose analysis frequencies $\{f_k\}$ closely spaced (see figure 2B).

Then $|f_k - f_0|$ is small for some value of k. Also, since the width of the lobes in figure 3 is $1/L_d$, where L_d is the delay weighting duration and will be taken of the order of the total record length available or utilized, very fine resolution in ν is possible. Hence, narrowband components closer than $1/L_w$, the resolution capability of a single time segment, can be resolved by using this technique.

FFT CONSIDERATIONS

Samples of the vernier spectrum $Y(f, \nu)$ were given in (9). The locations of the samples are†

$$\begin{aligned} f&: \ 0, \ \frac{1}{N\Delta}, \ \frac{2}{N\Delta}, \ \ldots, \ \frac{N-1}{N\Delta}; \\ \nu&: \ 0, \frac{1}{MS}, \ \frac{2}{MS}, \ \ldots, \ \frac{M-1}{MS} \ . \end{aligned} \tag{17}$$

The range covered by the vernier frequency ν is S^{-1}, and will be greater than the increment in f, which is $(N\Delta)^{-1}$, if overlapped temporal weighting is used. And since the full range, S^{-1}, would encompass a spurious lobe for values of $|f_0 - f|$ near $(2S)^{-1}$ (see figure 3), overlapping is necessary.

The approach adopted here is to utilize all the samples in f at separations of $(N\Delta)^{-1}$, and use only samples in ν which cover a range of $(N\Delta)^{-1}$; that is, we use the central portion of Y centered around $\nu = 0$, including negative frequencies. In terms of figure 2B, adjacent delay weightings at f_1, f_2, f_3 will be employed. The alternative time-saving procedure of attempting to utilize all of the M samples in ν, and using only enough samples in f to fill in the frequency axis, can lead to a very bad picket-fence effect, in addition to large spurious lobes at undesired frequency locations. These conclusions follow upon piecing together several vernier spectra like figure 3 for appropriate values of f and excitation frequency f_0.

---

*See reference 4, page 47.

†The upper half of the array of numbers in (17) corresponds to negative frequencies. Thus the last samples in each array correspond to $f = -(N\Delta)^{-1}$ and $\nu = -(MS)^{-1}$, respectively.

EXAMPLES

The general guidelines furnished in the previous section do not yet enable us to make quantitative selection of good weightings for different degrees of overlap. To make this selection, several examples are considered and compared. The numerical examples utilize

$$\Delta = \frac{1}{1024} \text{ seconds}, \quad N = 1024, \quad \frac{1}{MS} = \frac{1}{8} \text{ Hz}, \qquad f_0 = 256 \left(\frac{1}{16}\right) 256\frac{1}{2} \text{ Hz} . \tag{18}$$

(A sample program utilizing (9), (10), (11), (18), and the method of appendix A is given in appendix C for 75 percent overlap.)

50 PERCENT OVERLAP

At 50 percent overlap of the temporal weighting,* several possibilities were tried. They included

$$\left.\begin{array}{r} \text{cosine lobe} : \ w(t) = \cos(\pi t/L_w) \\ \text{cosine}^2 \text{ lobe (Hanning)} ; \ w(t) = \cos^2(\pi t/L_w) \\ \text{Dolph-Chebyshev (Reference 5)}\dagger \end{array}\right\} \ |t| < L_w/2 . \tag{19}$$

A complete list of cases is presented in table 1.

In figures 4A through 4I,‡ decibel plots of the magnitude of the estimated spectrum are given for cosine temporal weighting and for (cosine)^2 delay weighting. All plots are normalized with respect to a maximum of 0 dB, which occurs for $f_0 = f = 256$ Hz, $\nu = 0$ Hz. Figure 4A, for example, demonstrates the behavior predicted by figure 3, namely, the presence of spurious sidelobes every $S^{-1} = (.5 \times 1 \text{ s})^{-1} = 2$ Hz. The largest spurious lobe in figure 4A is -23.5 dB at 258 Hz. The slow rate of decay of the peaks at $256 \pm 2n$ Hz is due to the discontinuity of slope of w(t) at $\pm L_w/2$ for this example. The desirable feature of a narrow mainlobe is attained, as indicated in figure 4. The succession of plots in figure 4 shows that the extent of the picket fence varies greatly

*When these weightings are employed in the FFT, they are delayed by $L_w/2$ seconds, thereby being nonzero in the interval (0, L_w).

†A quick and accurate method of generating the Dolph-Chebyshev weights by means of efficient use of an FFT is presented in reference 6.

‡Figures 4 through 14 follow the text, beginning on page 16.

Table 1. Examples of Temporal and Delay Weightings

Figure	Temporal Weighting	Delay Weighting	Overlap (%)	Number of Tones
4	cosine	cosine^2	50	1
5	cosine^2	cosine^2	50	1
6	Dolph-Chebyshev	cosine^2	50	1
7	cosine^2	cosine^2	75	1
8	cosine^3	cosine^2	75	1
9	cosine^4	cosine^2	75	1
10	cosine^5	cosine^2	75	1
11	Dolph-Chebyshev	cosine^2	75	1
12	cosine^2	flat	75	1
13	cosine^2	cosine^2	75	2
14	cosine^2	flat	75	2

with excitation frequency, reaching a maximum of -3.20 dB in figure 4H for f_0 = 256 7/16 Hz. (The figures for f_0 > 256 1/2 Hz repeat the behavior shown.) The worst sidelobe of -23.0 dB occurs for f_0 = 256 1/8 Hz, as shown in figure 4C.

It should be noted that if sidelobes were to be measured with respect to the peak on that same plot, figure 4C would yield a sidelobe of -23.0 + 0.13 = -22.9 dB. Thus, the convention adopted here must be kept in mind in the following discussion.

Instead of applying the weighting directly in the time domain by means of multiplication on the data x, the effect of cosine weighting can be accomplished in the frequency domain by means of convolution of the spectrum with the sequence $(1/2)\{1, -1\}$; however, the resultant must be interpreted as the spectral value between the two quantities convolved at each frequency step. * More generally, $(\text{cosine})^n$ time weighting can be accomplished alternatively by means of convolution of the (unweighted) spectrum with the sequence

$$\left(\frac{1}{2}\right)^n \left\{1, -n, \binom{n}{2}, -\binom{n}{3}, \ldots, (-1)^n\right\} \qquad (20)$$

*This possibility and its interpretation were pointed out by Dr. N. L. Owsley.

of length $n + 1$, and then interpreted as the spectral value at the center of the region convolved, for each frequency step; see appendix D. The convolutional sequences in (20) are given in table 2 for $n = 1$ through 5.

Table 2. Convolution Sequences

n	Convolution Sequence
1	$i\ 1/2\{1, -1\}$
2	$1/4\{-1, 2, -1\}$
3	$i\ 1/8\{-1, 3, -3, 1\}$
4	$1/16\{1, -4, 6, -4, 1\}$
5	$i\ 1/32\{1, -5, 10, -10, 5, -1\}$

Since the effect of $(\text{cosine})^2$ temporal weighting is very easy to incorporate in the frequency domain by means of convolution, it must be considered as a candidate for weighting. The results in figures 5A and 5B show that although the picket fence is reduced to -2.70 dB, the peak sidelobe increases to -15.4 dB. (For brevity, we are now presenting only selected cases of worst excitation frequencies.) The reason for the increased sidelobes for this temporal weighting is that 50 percent overlap is not yet great enough to realize the deeper first sidelobe level of -31.5 dB; that is, we are still sampling, according to figure 3, on the skirts of the mainlobe for some excitation frequencies. Generally, for 50 percent overlap, the peak sidelobe will occur approximately at the excitation frequency such that the worst sidelobe (or mainlobe) of the temporal window beyond $f = 1.5/L_W$ is encountered; this may be seen by considering figure 3 and recalling that we plot only the central portion of $Y(f, \nu)$. Thus the $(\text{cosine})^n$ weightings in tables 1 and 2 for $n > 2$ are not acceptable for 50 percent overlap, since sampling of the mainlobe is encountered.

The realization of minimum sidelobe level for a specified beamwidth (to the first null) is exactly the problem addressed by Dolph, reference 5. Accordingly, this weighting is of considerable importance in spectral estimation. In figures 6A-6C, the effects of Dolph-Chebyshev time weighting are presented. The worst sidelobe of -33.2 dB occurs for $f_0 = 256\ 1/8$ Hz (figure 6C). These results are noticeably better than in figures 4 and 5.

When triangular temporal weighting was tried, it had a peak sidelobe of -20.2 dB; again, we are sampling the skirts of the mainlobe. Thus, if 50 percent overlap is all that can be utilized for some applications, due perhaps to limited computation time, the cosine-lobe temporal weighting is the best of the simply applied windows (that is, by means of frequency domain convolution), but the Dolph-Chebyshev time weighting is 10 dB better than the cosine lobe weighting.

75 PERCENT OVERLAP

At 75 percent overlap of the temporal weightings the following examples were utilized:

$$\left.\begin{array}{ll} \text{cosine}^2 \text{ lobe (Hanning)} & : w(t) = \cos^2 (\pi t/L_W) \\ \text{cosine}^3 \text{ lobe} & : w(t) = \cos^3 (\pi t/L_W) \\ \text{cosine}^4 \text{ lobe} & : w(t) = \cos^4 (\pi t/L_W) \\ \text{cosine}^5 \text{ lobe} & : w(t) = \cos^5 (\pi t/L_W) \\ \text{Dolph-Chebyshev} & \text{----} \end{array}\right\} |t| < L_W/2 . \qquad (21)$$

The results for the Hanning weighting are given in figure 7. The peak sidelobe is -41.8 dB at f_O = 256 1/2 Hz in figure 7C, and the picket fence is -2.60 dB at f_O = 256 7/16 Hz in figure 7B. Thus, a much improved sidelobe level is realized relative to 50 percent overlap, at the expense of increased computation effort, that is, increased overlap and number of FFTs.

In an effort to further improve performance, the (cosine)^3 weighting, which has a higher degree of continuous derivatives at $\pm L_W/2$, was tried. The results in figure 8 show a maximum sidelobe of -51.2 dB and a picket fence of -2.34 dB.

Continuation of this effort to smoother weightings such as (cosine)^4, figure 9, shows a peak sidelobe of -48.1 dB and a picket fence of -2.18 dB. The peak sidelobe has increased over that for (cosine)^3 weighting because, for 75 percent overlap, the peak sidelobe (or main lobe) of the temporal window beyond approximately $f = 3.5/L_W$ is encountered. It so happens that the worst case in this region is larger for (cosine)^4 than for (cosine)^3 temporal weighting.

For (cosine)^5 temporal weighting, the peak sidelobe is reduced further to -54.1 dB. Also, the picket fence is improved to -2.07 dB; see figure 10. This weighting is easily accomplished via frequency domain manipulations; see table 2. An alternative temporal weighting of virtually equal quality to (cosine)^5 is cubic, that is, sections of cubic curves that have continuous derivatives of as high order as possible. The temporal window is proportional to

$$\left[\frac{\sin (\pi L_W f/4)}{\pi L_W f/4}\right]^4 \qquad (22)$$

and has a worst sidelobe of -53.1 dB. (The picket fence was not computed.) However, a cubic temporal weighting is not easily accomplished in the frequency domain.

When (cosine)^6 temporal weighting is considered, it is found that 75 percent overlap forces us to sample the temporal window on the skirts of its mainlobe. This is an unacceptable weighting because the peak sidelobe in the vernier spectrum increases significantly.

The possibilities of Dolph-Chebyshev weighting are indicated in figure 11. The worst sidelobe is -86 dB in figure 11B for f_0 = 256 1/4 Hz, and the picket fence is -2.29 dB in figure 11C for f_0 = 256 7/16 Hz. This is a 32-dB improvement in sidelobe level compared with (cosine)^5 weighting. The picket fence is degraded by 0.22 dB.

To determine the effect of not using delay weighting, figure 12 was computed for (cosine)^2 temporal weighting and flat delay weighting. For certain excitation frequencies, a very narrow mainlobe is realized; see figure 12A. However, for other excitation frequencies, the lack of delay weighting creates broad "shoulders" of significant level; see figure 12B. Also, the sampling in f and ν, inherent in the FFT, produces a picket fence of -5.0 dB. Thus, although a low peak sidelobe is attained, lack of delay weighting is very detrimental to performance, as will be further demonstrated below. Notice from figure 7 that (cosine)^2 delay weighting also yields a peak sidelobe of -41.8 dB, but has no broad shoulders and has a picket fence of only -2.60 dB.

The detrimental effects of no delay weighting are best illustrated by a comparison of figures 13 and 14, which have two tones separated by 1/2 Hz, one 15 dB stronger than the other. It is seen that these two tones are resolved, even though they are closer than the resolution capability of the individual time segments, that is, closer than 1 Hz. In figure 13, (cosine)^2 delay weighting is employed; in figure 14, none is employed. A comparison of part A of these figures reveals that, for excitation frequencies 256 and 256 1/2 Hz, the flat delay weighting is better. However, for excitation frequencies 256 1/16 and 256 9/16 Hz, the presence of the weaker tone is clearly evident in figure 13B, but hardly discernible in figure 14B (no delay weighting). The presence of noise would obscure the weaker peak. Thus, although the peak sidelobe may be very small, the presence of high-level broad shoulders must also be eliminated by use of delay weighting.

CONCLUSIONS

An approximate and quick FFT technique for vernier spectral analysis is possible by employing overlapped temporal weighting and delay weighting. For 50 percent overlap and Hanning delay weighting, the best simply-applied temporal weighting discovered was a single cosine lobe, realizing a peak sidelobe

of -23 dB. However, Dolph-Chebyshev temporal weighting achieves -33 dB sidelobes. For 75 percent overlap and Hanning delay weighting, the best simply applied temporal weighting discovered was (cosine)^5, which realized a peak sidelobe of -54 dB. However, Dolph-Chebyshev temporal weighting is capable of -86 dB sidelobes. Which overlap and weighting to employ depends on the limitations on computation time and storage, and on the relative strength and location of interfering tones.

The overlap is not limited to the above choices. It could, for example, be 67 percent. The best weightings were not investigated in this case, because it was felt that the above overlaps were easier to implement in most cases of practical interest. However, Dolph-Chebyshev weighting is always a strong candidate and is quickly and accurately generated (reference 6).

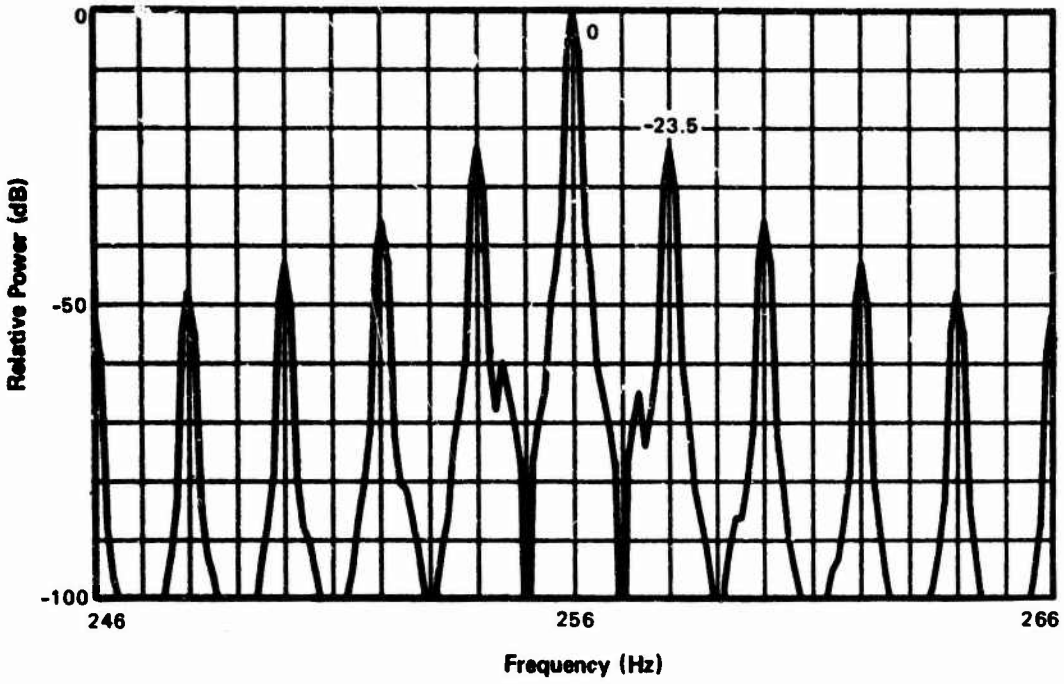

Figure 4A. f_o = 256 Hz

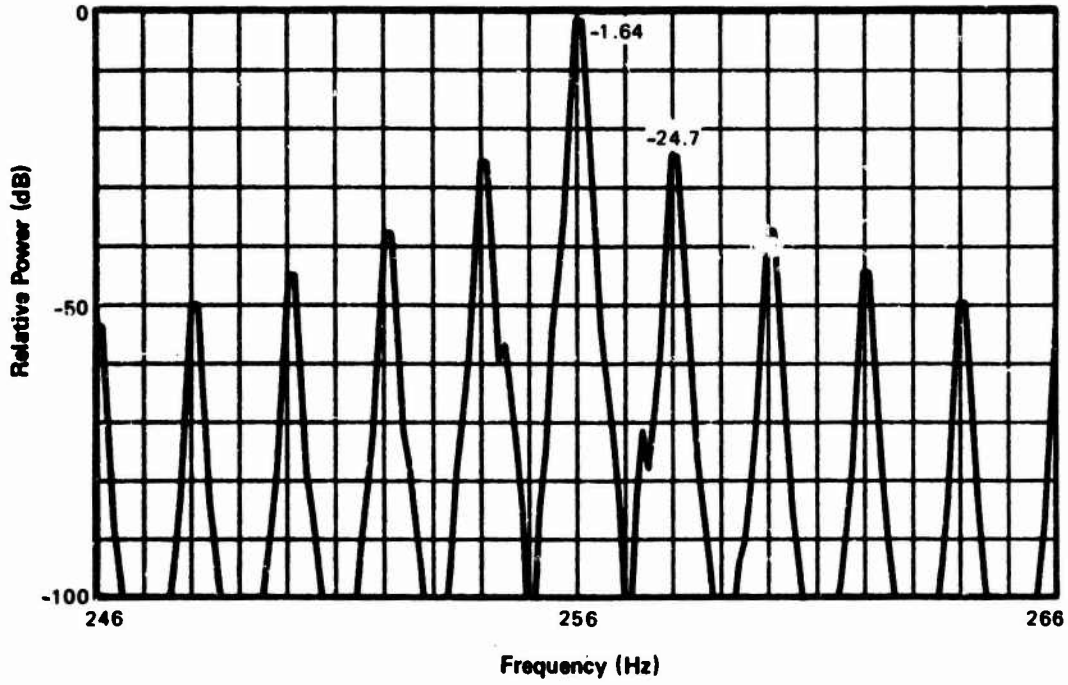

Figure 4B. f_o = 256 1/16 Hz

Figure 4. Vernier Spectrum for Cosine Temporal Weighting, 50 percent Overlap

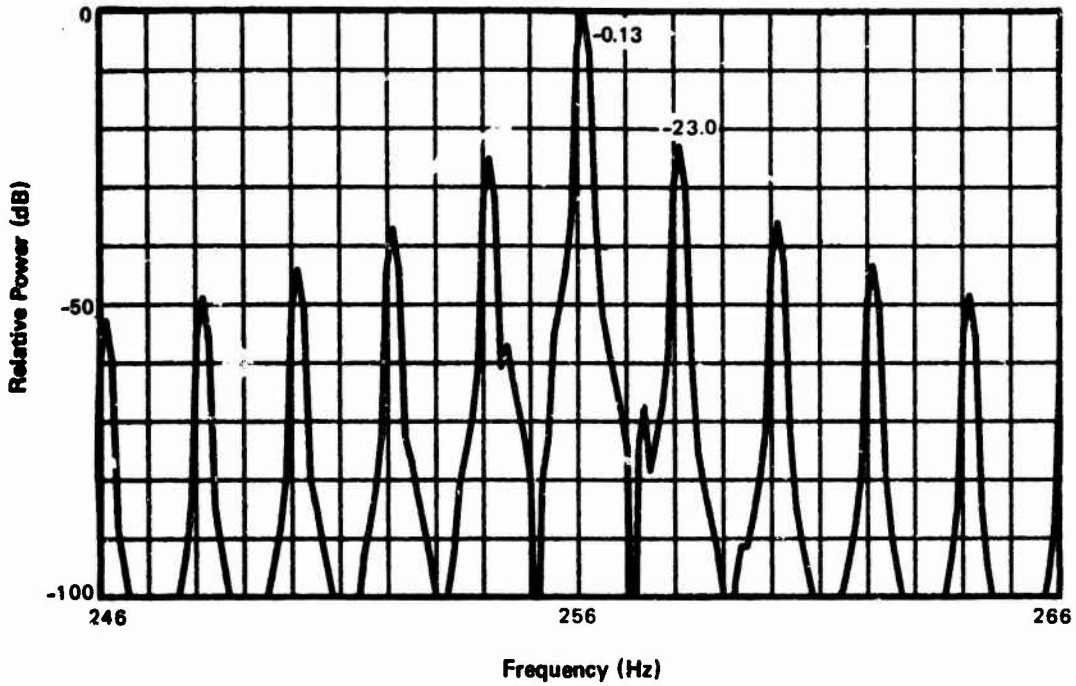

Figure 4C. f_0 = 256 2/16 Hz

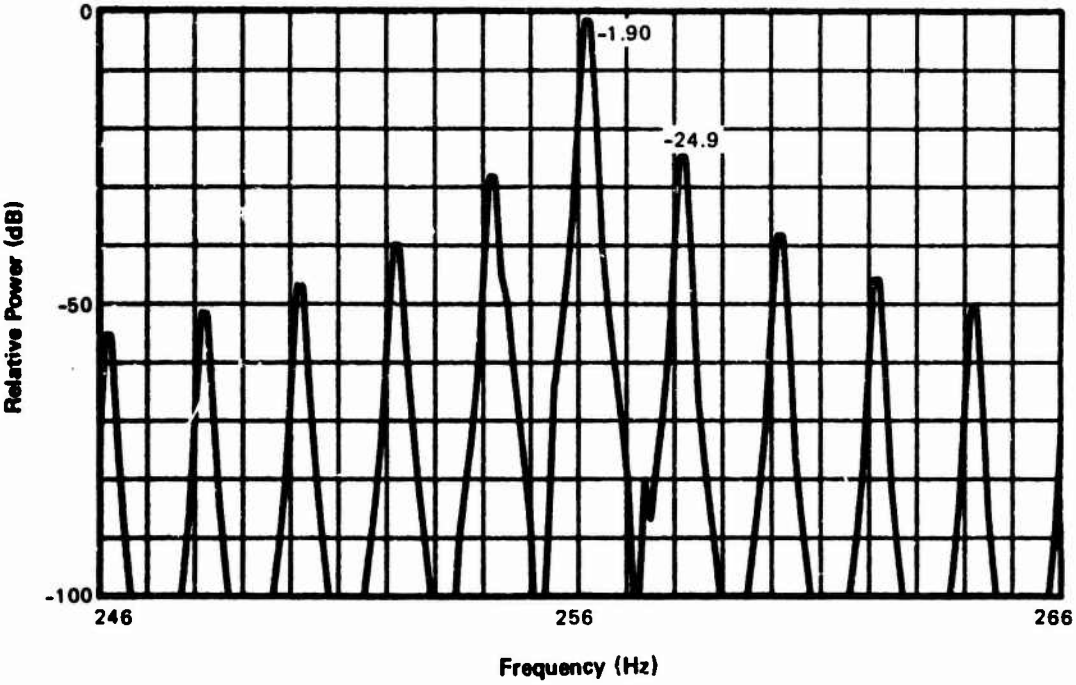

Figure 4D. f_0 = 256 3/16 Hz

Figure 4 (Cont'd). Vernier Spectrum for Cosine Temporal Weighting, 50 percent Overlap

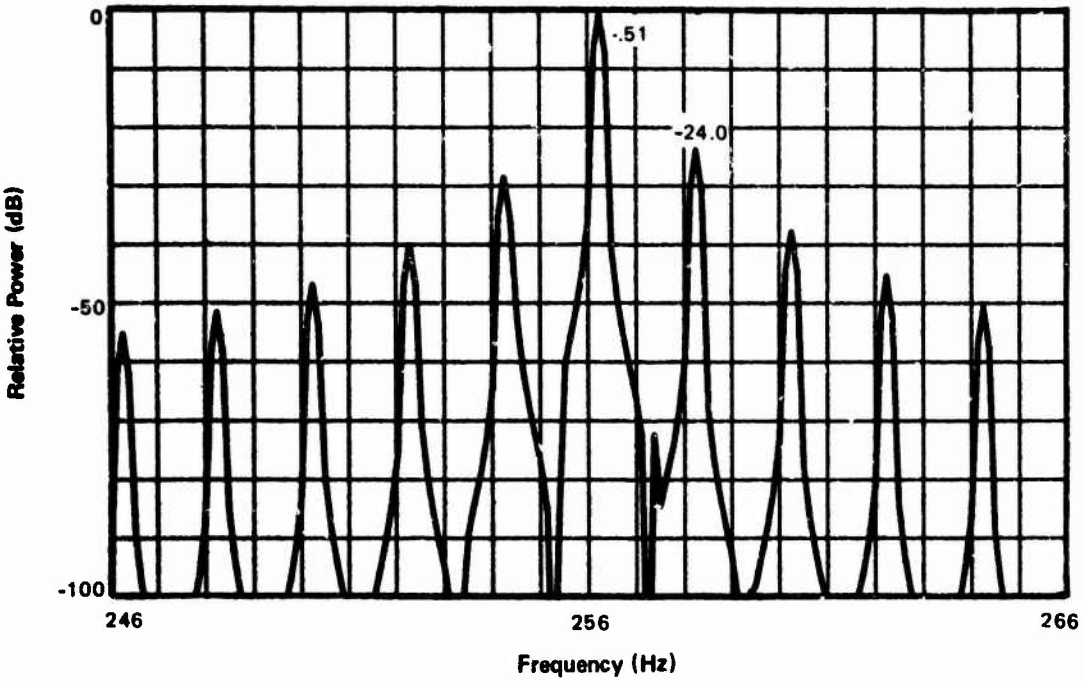

Figure 4E. f_o = 256 4/16 Hz

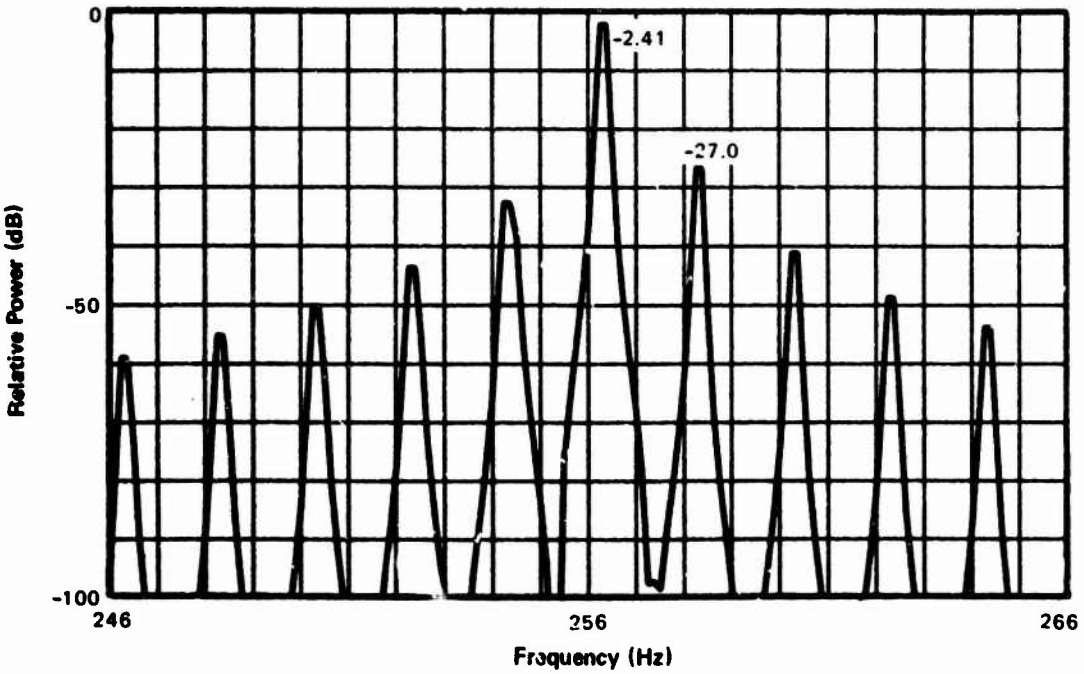

Figure 4F. f_o = 256 5/16 Hz

Figure 4 (Cont'd). Vernier Spectrum for Cosine Temporal Weighting, 50 percent Overlap

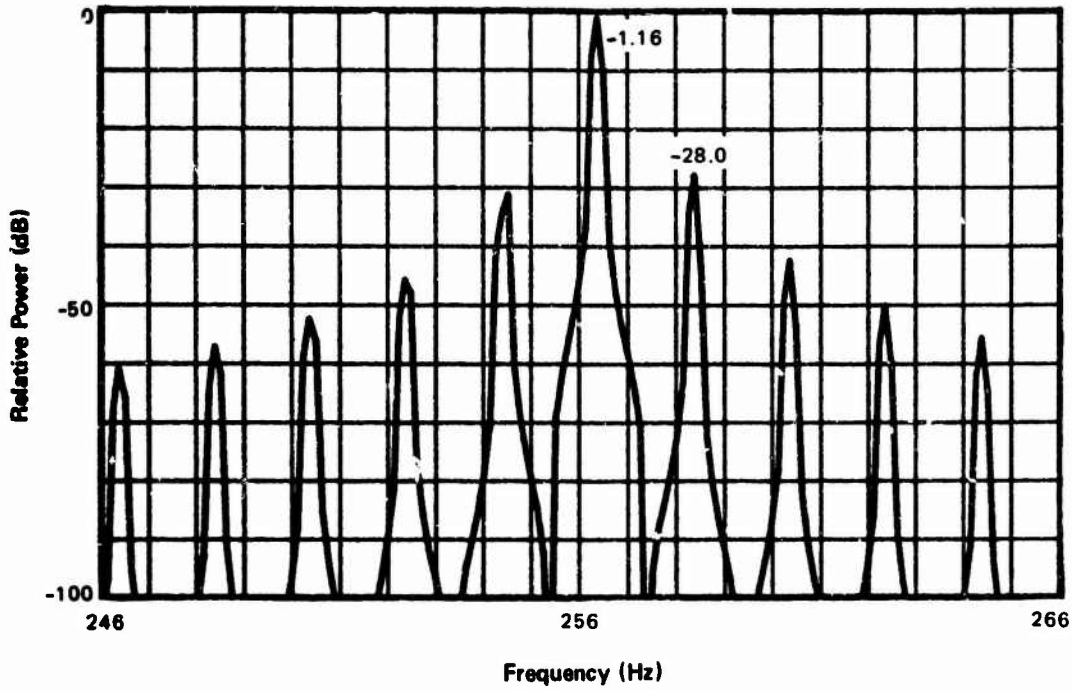

Figure 4G. f_0 = 256 6/16 Hz

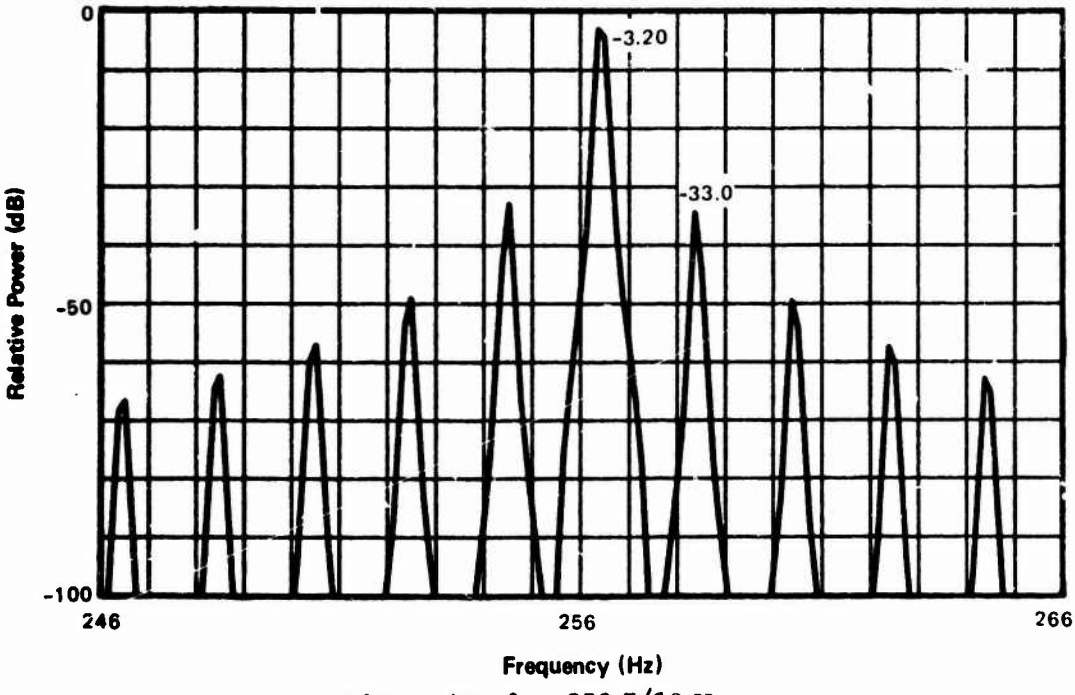

Figure 4H. f_0 = 256 7/16 Hz

Figure 4 (Cont'd). Vernier Spectrum for Cosine Temporal Weighting, 50 percent Overlap

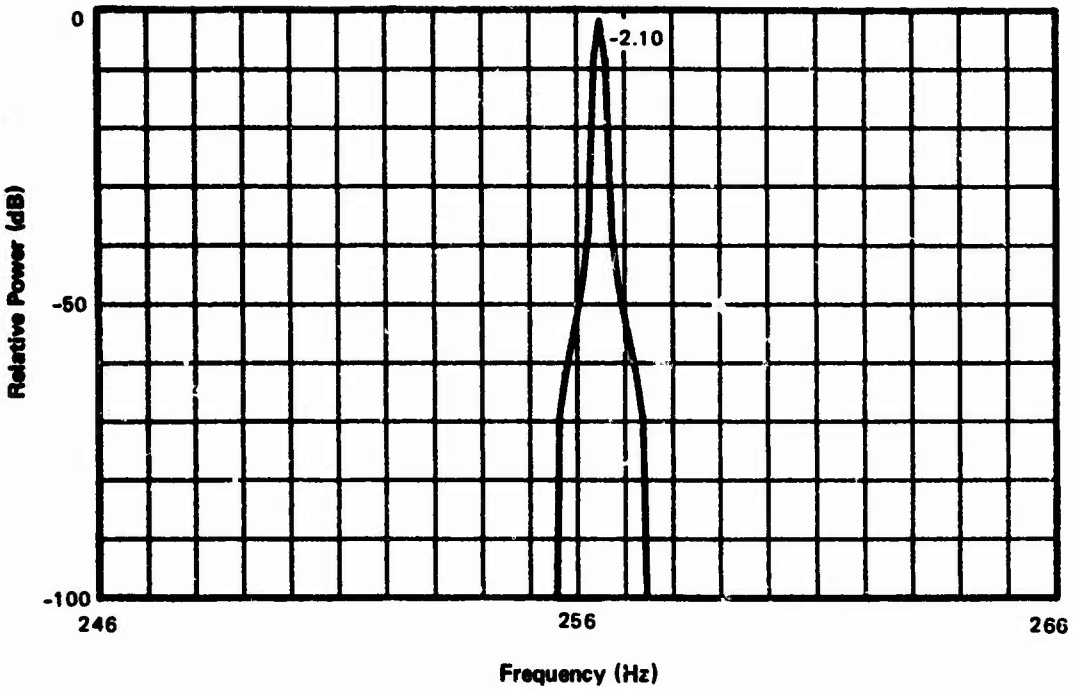

Figure 4I. f_0 = 256 1/2 Hz

Figure 4 (Cont'd). Vernier Spectrum for Cosine Temporal Weighting, 50 percent Overlap

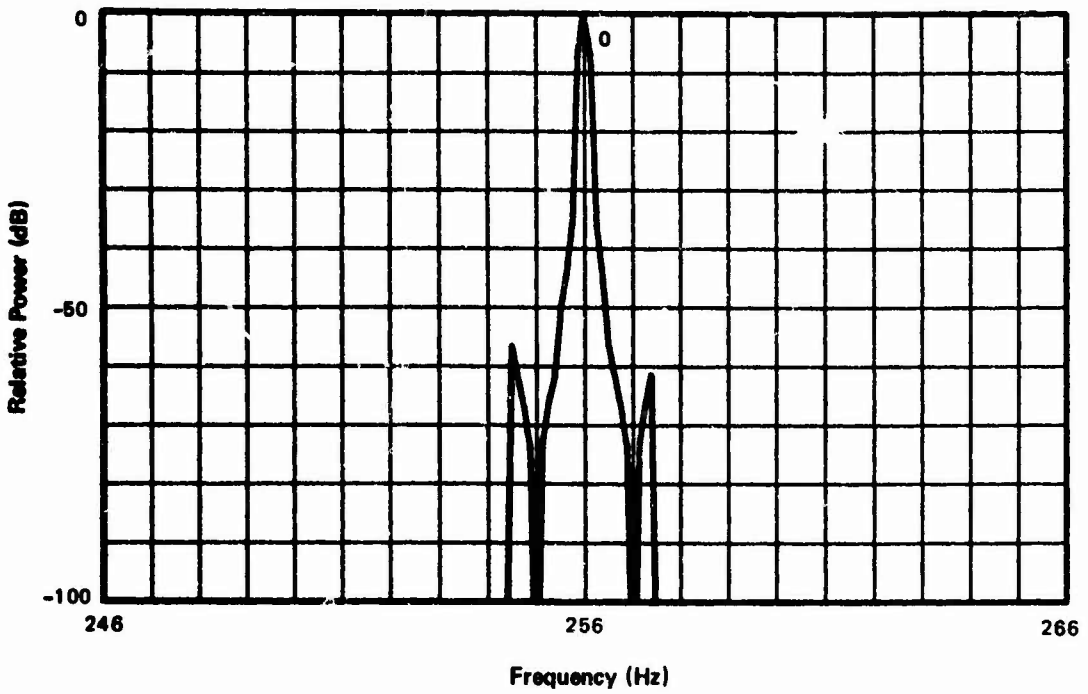

Figure 5A. f_o = 256 Hz

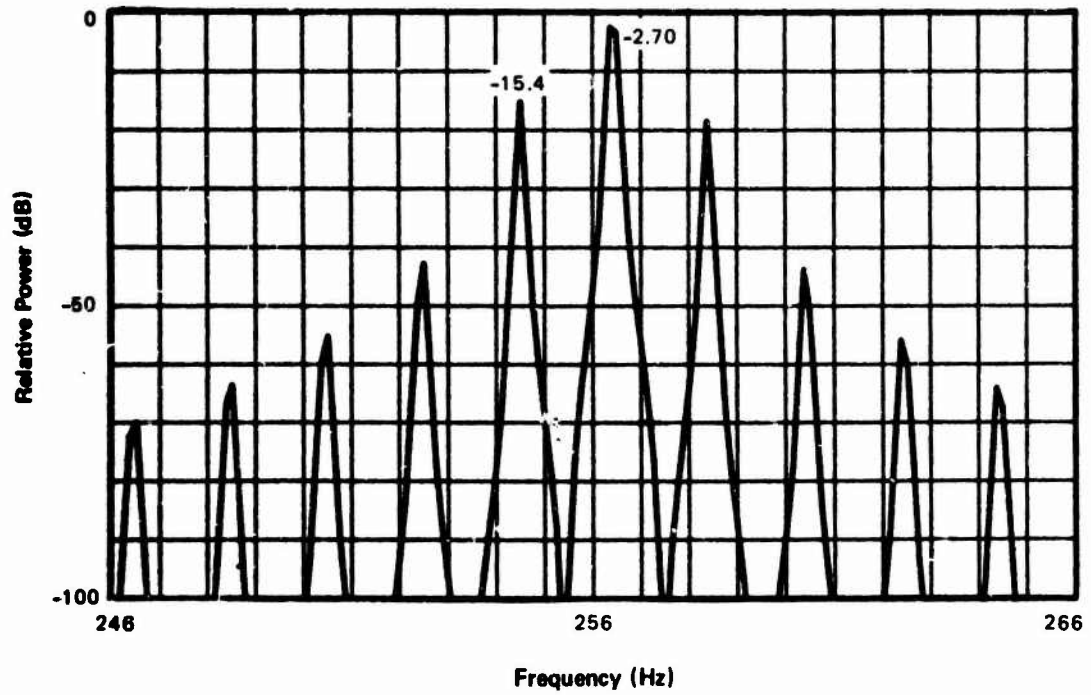

Figure 5B. f_o = 256 7/16 Hz

Figure 5. Vernier Spectrum for (Cosine)^2 Temporal Weighting, 50 percent Overlap

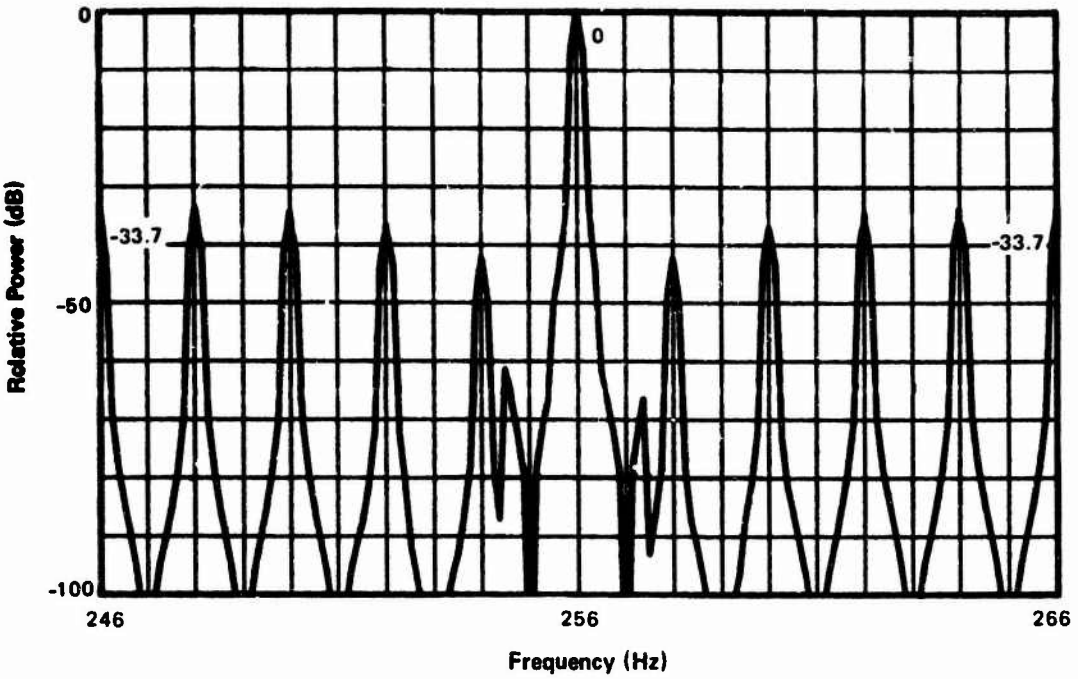

Figure 6A. f_o = 256 Hz

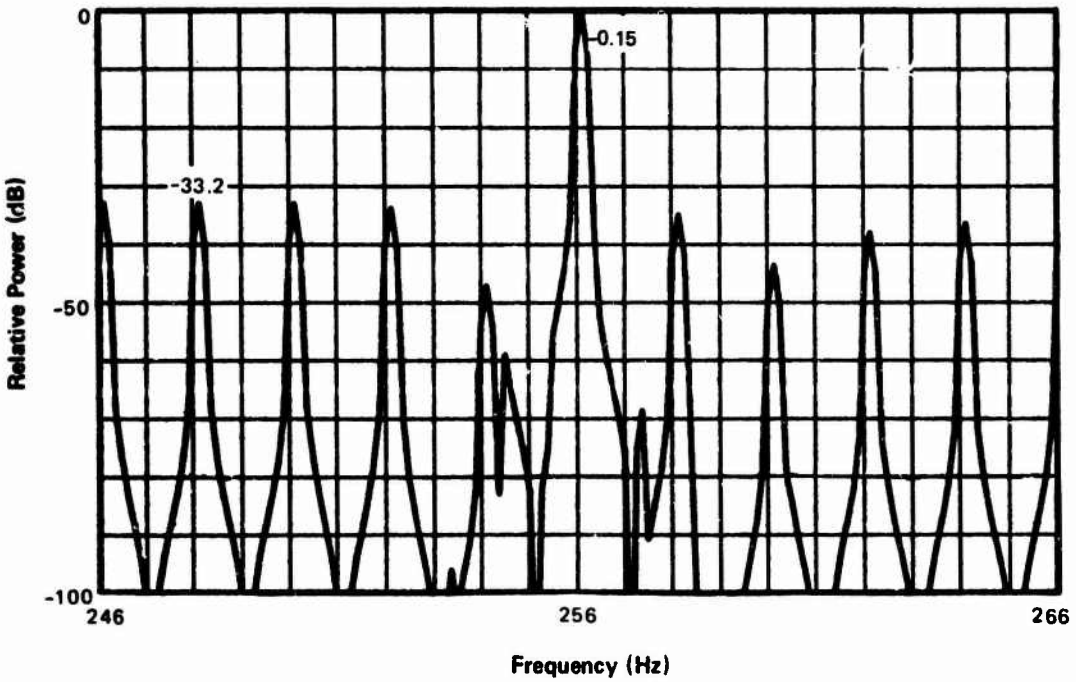

Figure 6B. f_o = 256 1/8 Hz

Figure 6. Vernier Spectrum for Dolph-Chebyshev Temporal Weighting, 50 percent Overlap

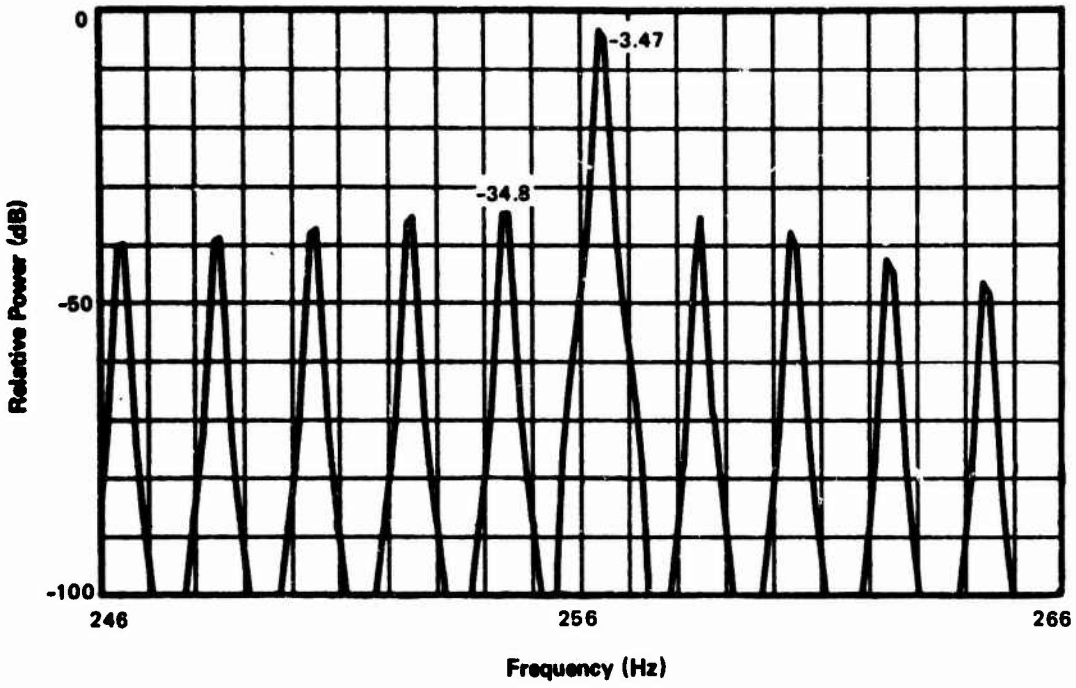

Figure 6C. f_o = 256 7/16 Hz

Figure 6 (Cont'd). Vernier Spectrum for Dolph-Chebyshev Temporal Weighting, 50 percent Overlap

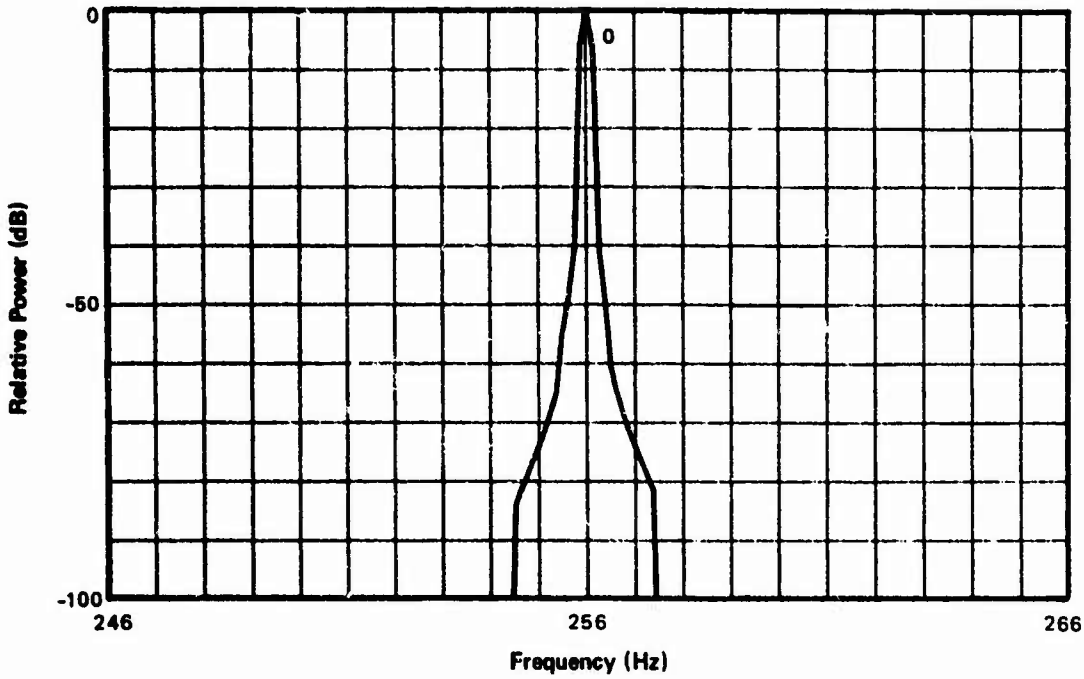

Figure 7A. f_o = 256 Hz

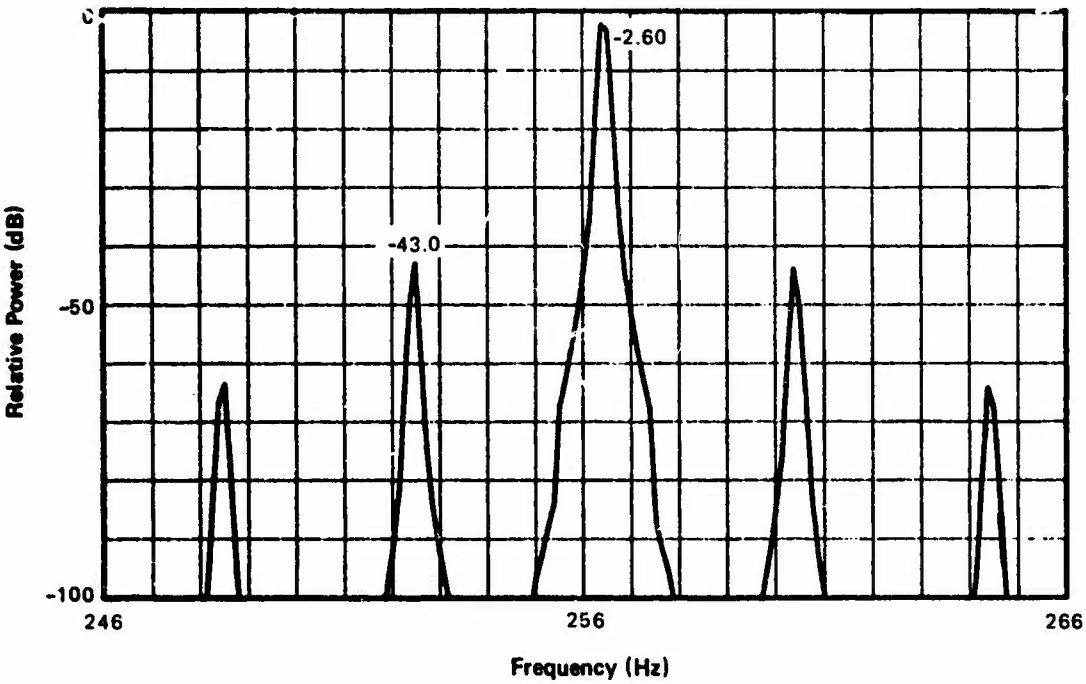

Figure 7B. f_o = 256 7/16 Hz

Figure 7. Vernier Spectrum for (Cosine)^2 Temporal Weighting, 75 percent Overlap

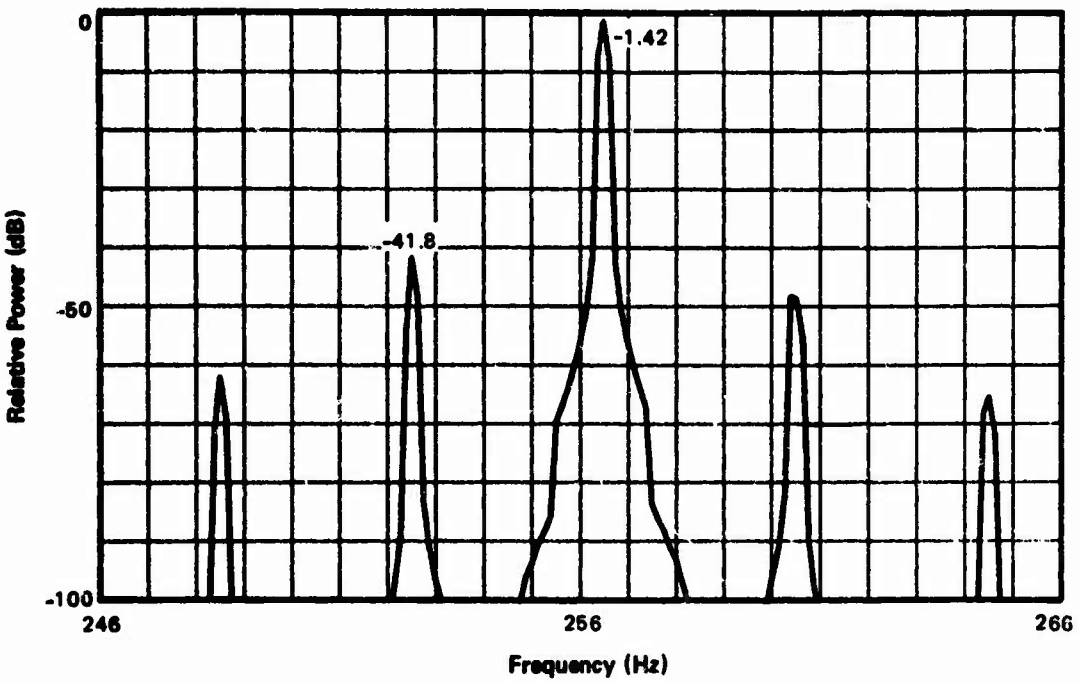

Figure 7C. f_o = 256 1/2 Hz

Figure 7 (Cont'd). Vernier Spectrum for (Cosine)^2 Temporal Weighting, 75 percent Overlap

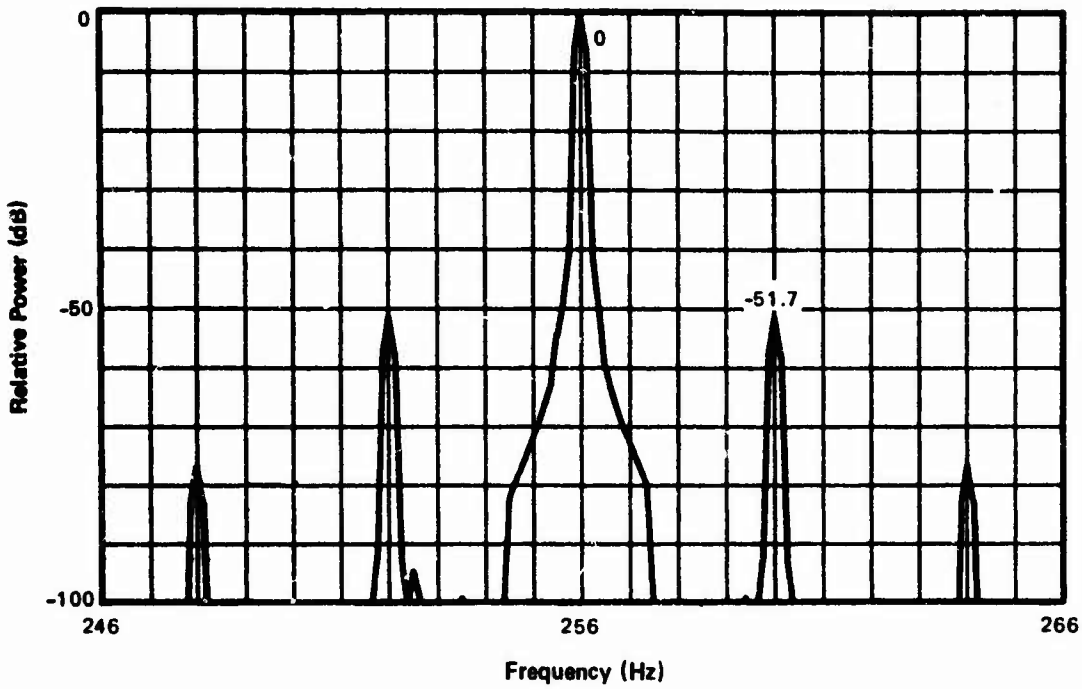

Figure 8A. f_0 = 256 Hz

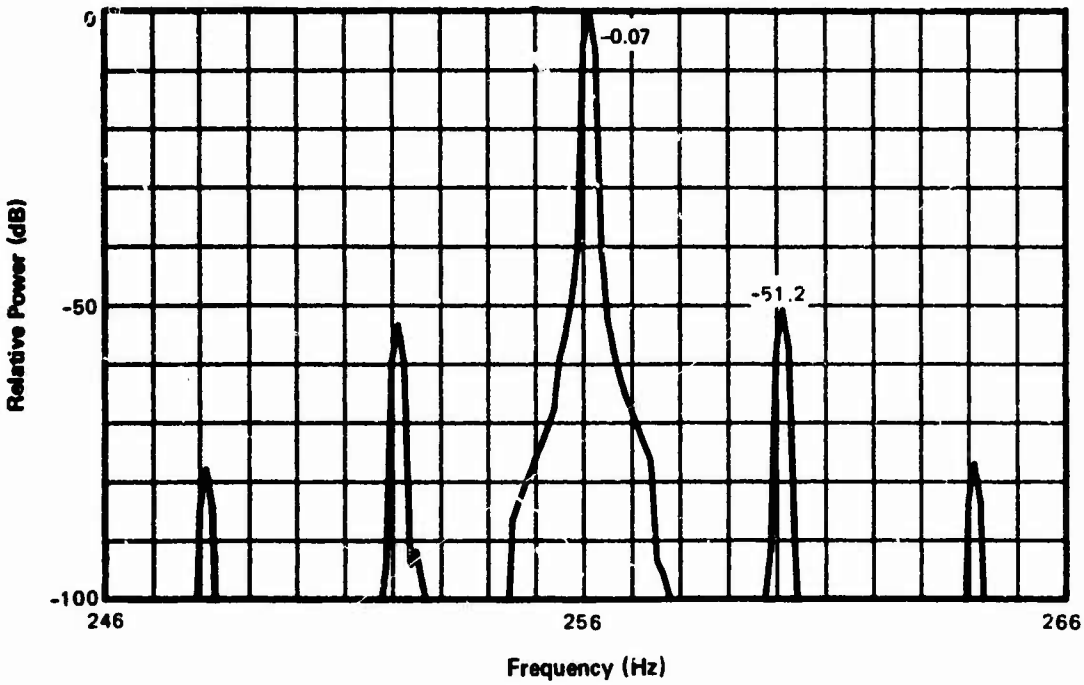

Figure 8B. f_0 = 256 1/8 Hz

Figure 8. Vernier Spectrum for (Cosine)^3 Temporal Weighting, 75 percent Overlap

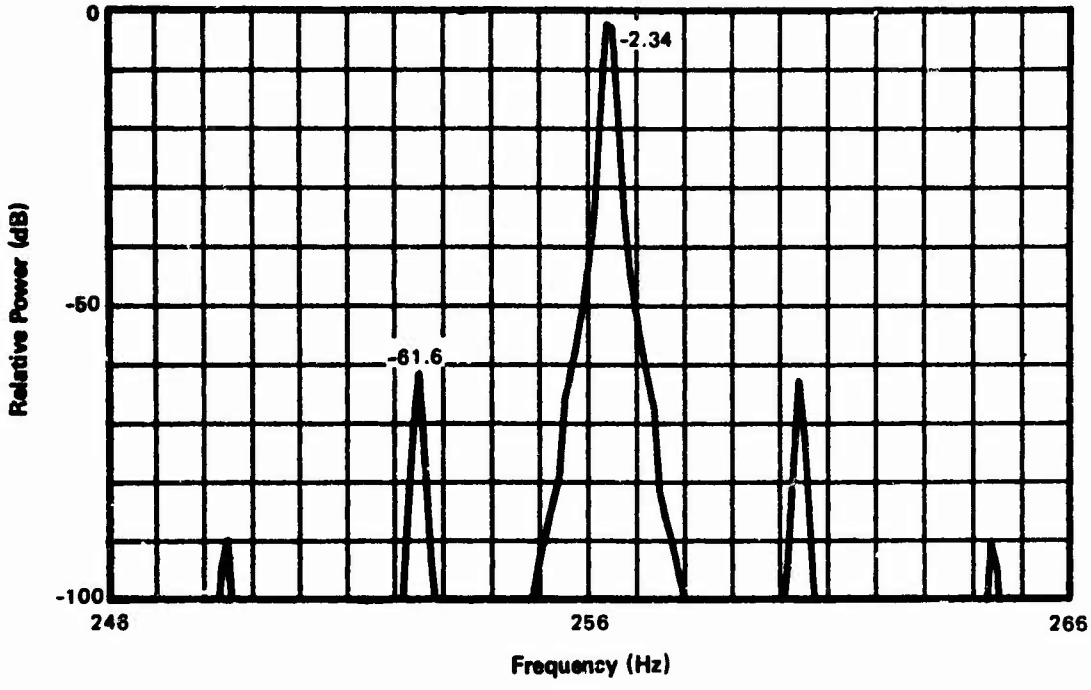

Figure 8C. f_o = 256 7/16 Hz

Figure 8 (Cont'd). Vernier Spectrum for (Cosine)^3 Temporal Weighting, 75 percent Overlap

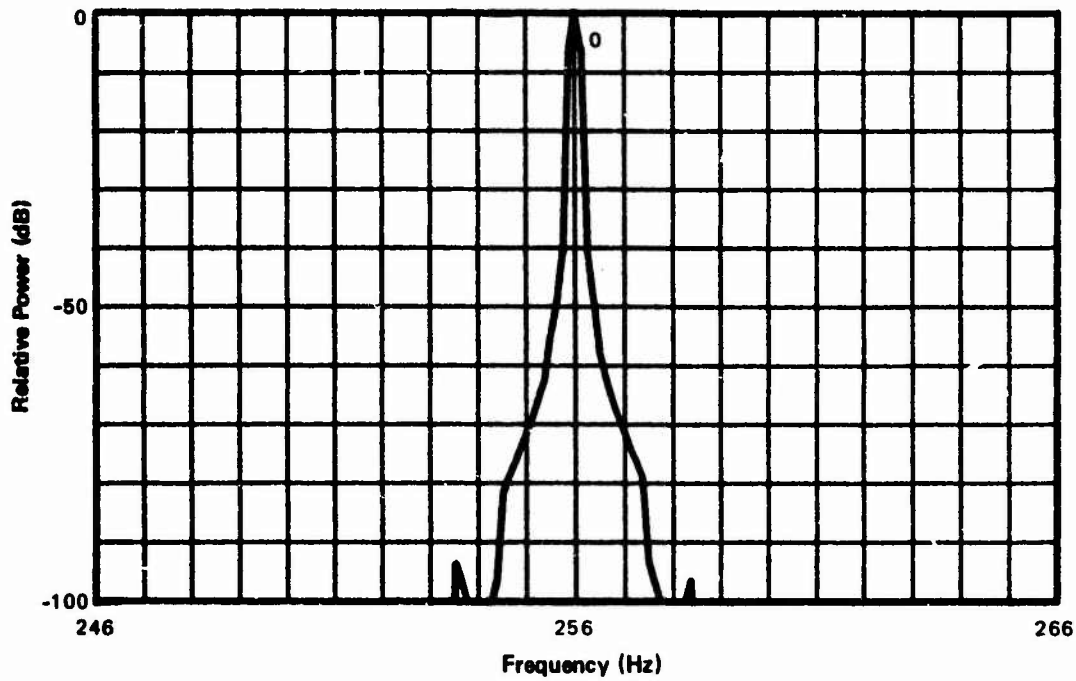

Figure 9A. f_o = 256 Hz

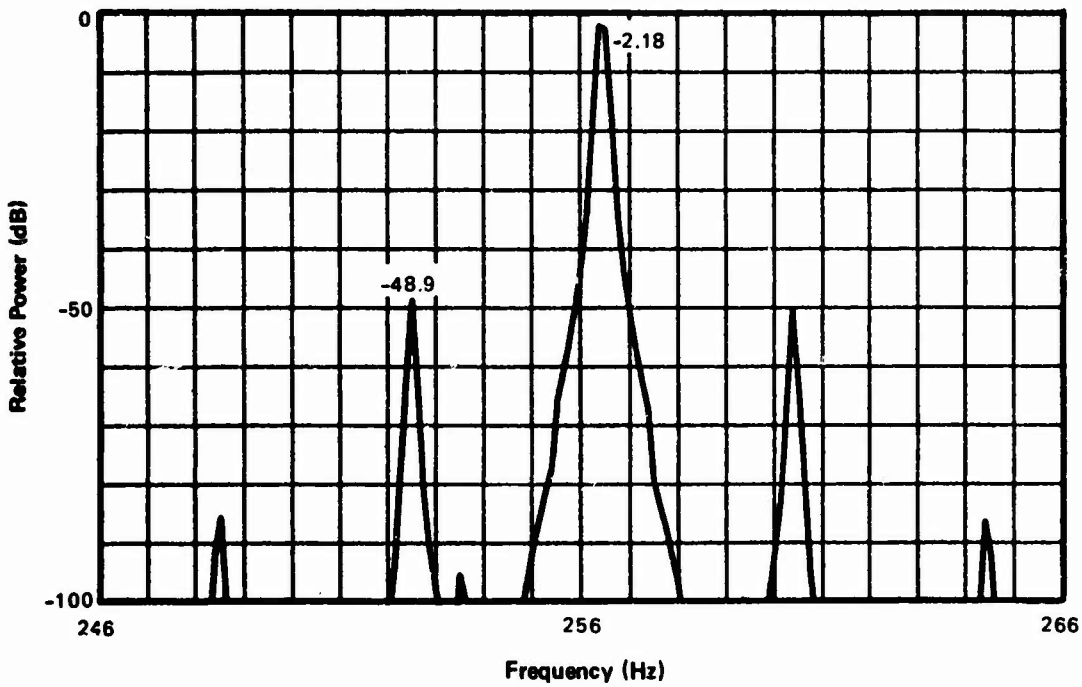

Figure 9B. f_o = 256 7/16 Hz

Figure 9. Vernier Spectrum for (Cosine)^4 Temporal Weighting, 75 percent Overlap

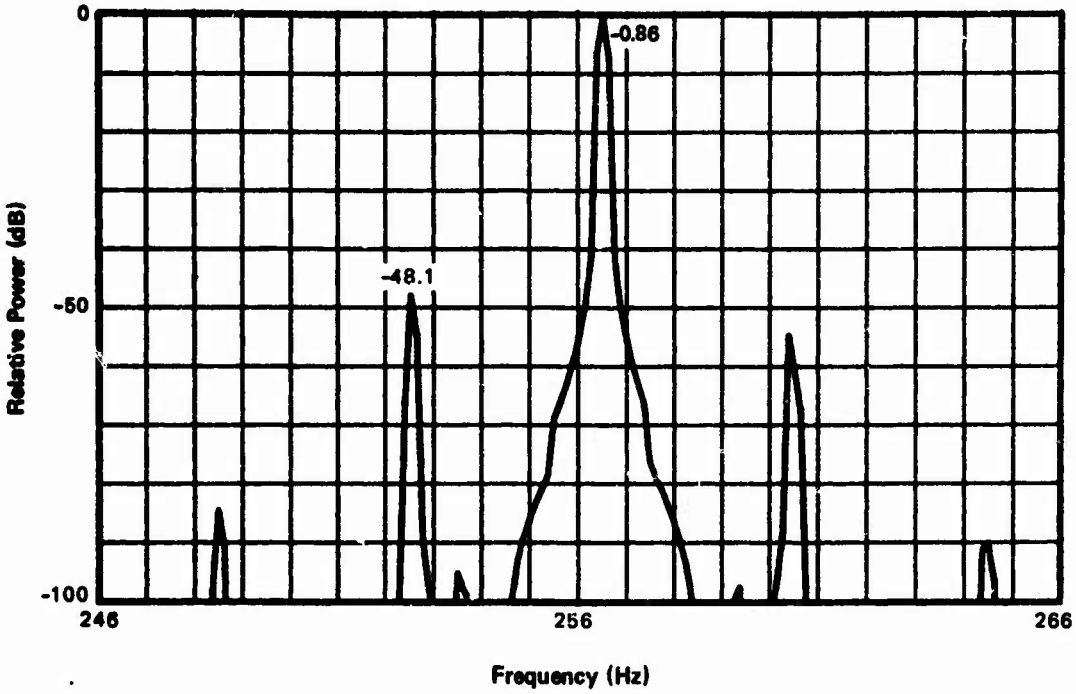

Figure 9C. f_o = 256 1/2 Hz

Figure 9 (Cont'd). Vernier Spectrum for (Cosine)^4 Temporal Weighting, 75 percent Overlap

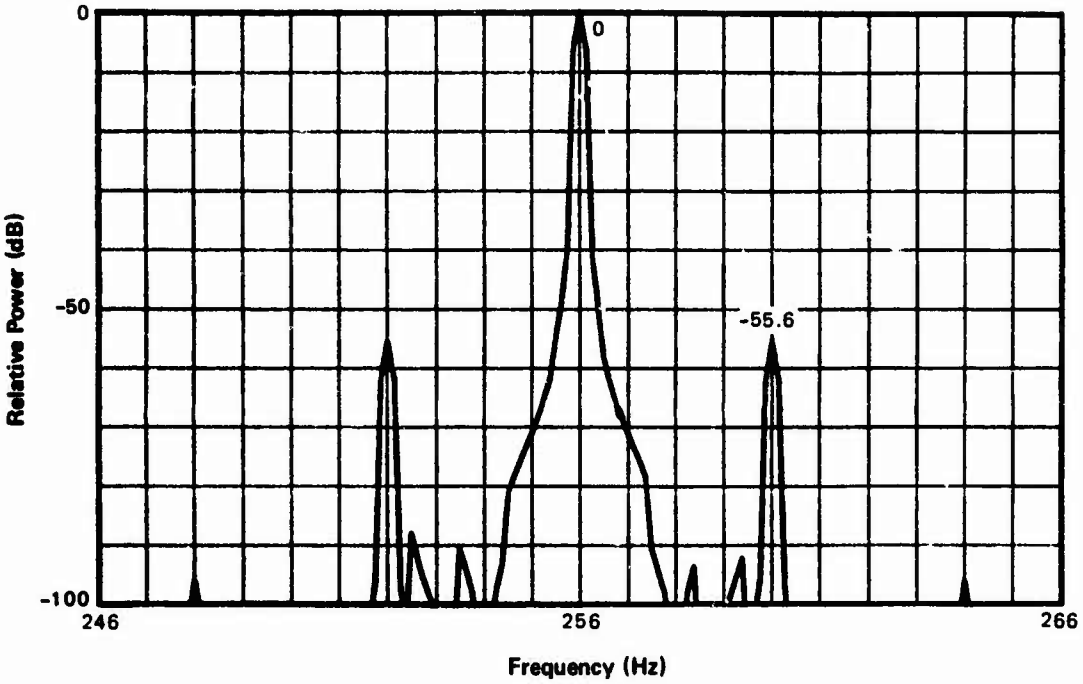

Figure 10A. f_0 = 256 Hz

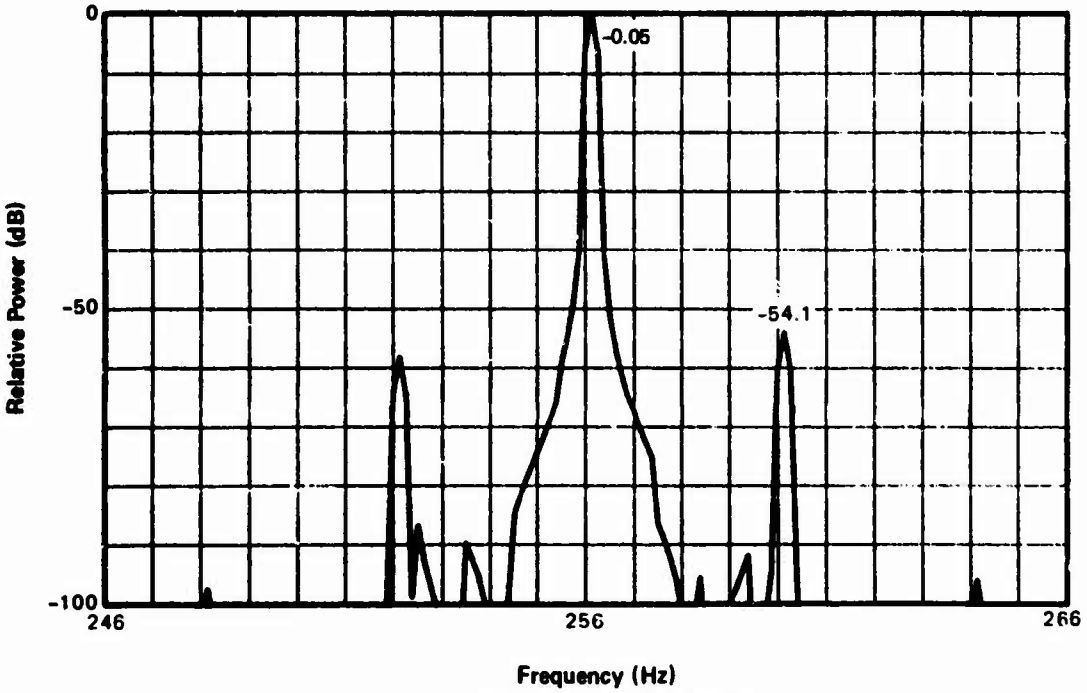

Figure 10B. f_0 = 256 1/8 Hz

Figure 10. Vernier Spectrum for (Cosine)^5 Temporal Weighting, 75 percent Overlap

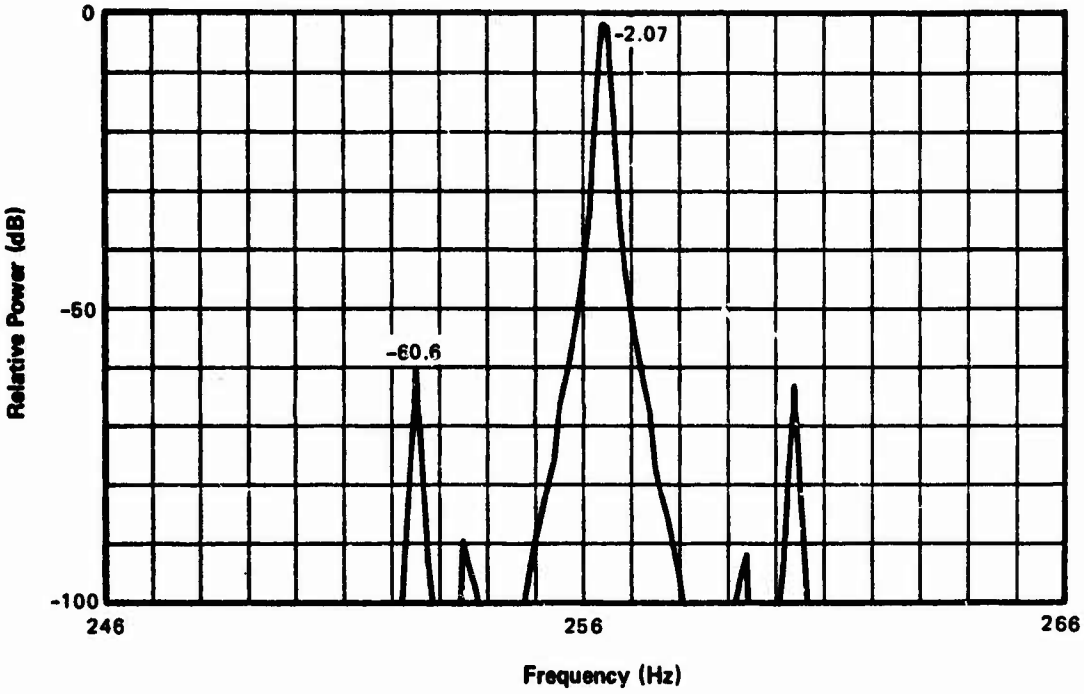

Figure 10C. f_0 = 256 7/16 Hz

Figure 10 (Cont'd). Vernier Spectrum for (Cosine)^5 Temporal Weighting, 75 percent Overlap

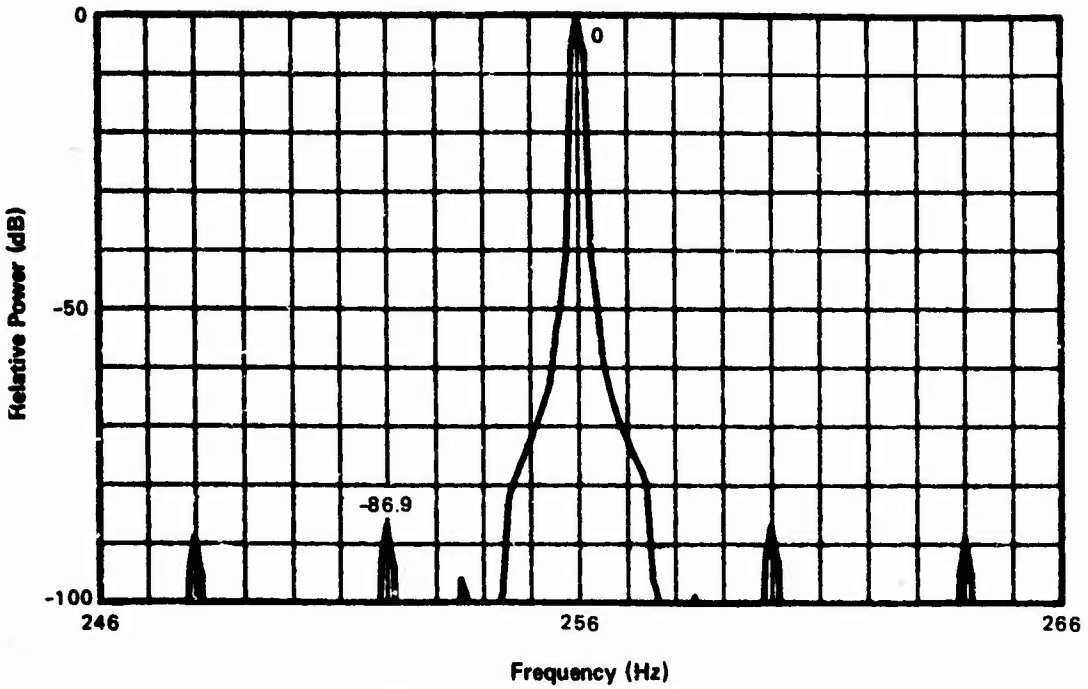

Figure 11A. f_0 = 256 Hz

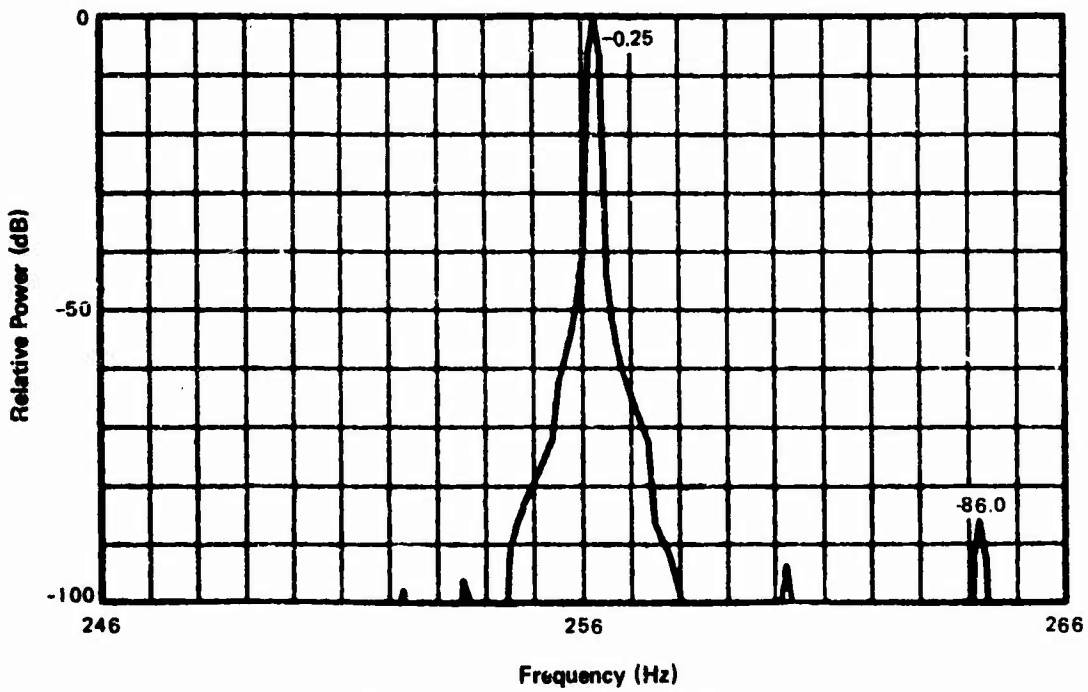

Figure 11B. f_0 = 256 1/4 Hz

Figure 11. Vernier Spectrum for Dolph-Chebyshev Temporal Weighting, 75 percent Overlap

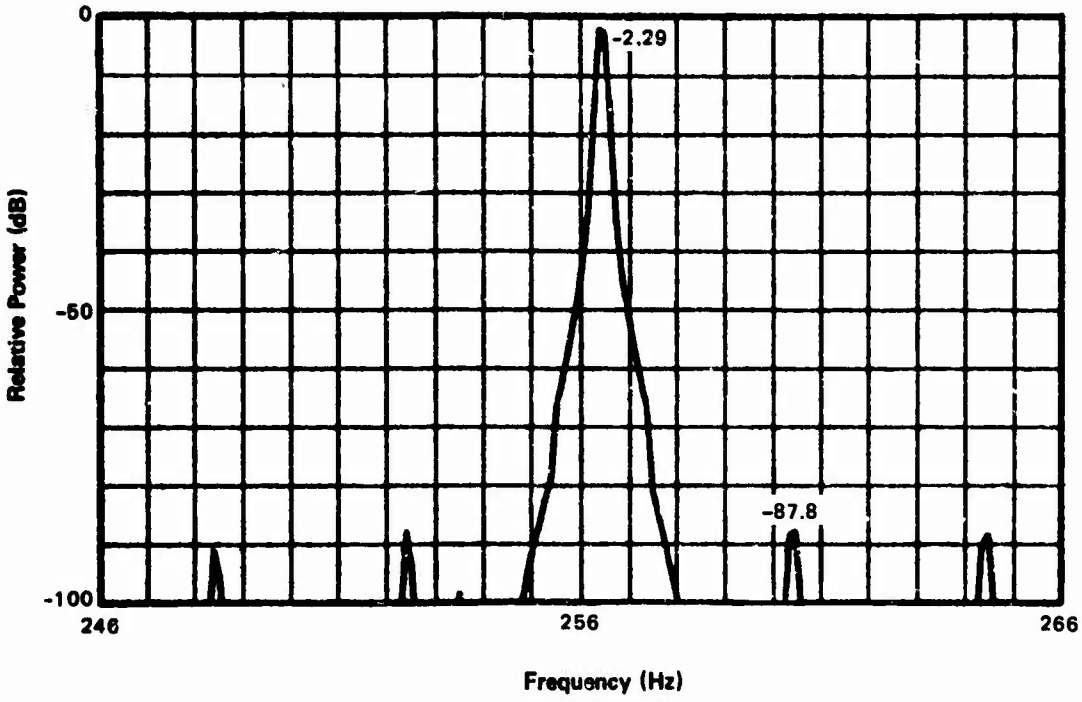

Figure 11C. f_0 = 256 7/16 Hz

Figure 11 (Cont'd). Vernier Spectrum for Dolph-Chebyshev Temporal Weighting, 75 percent Overlap

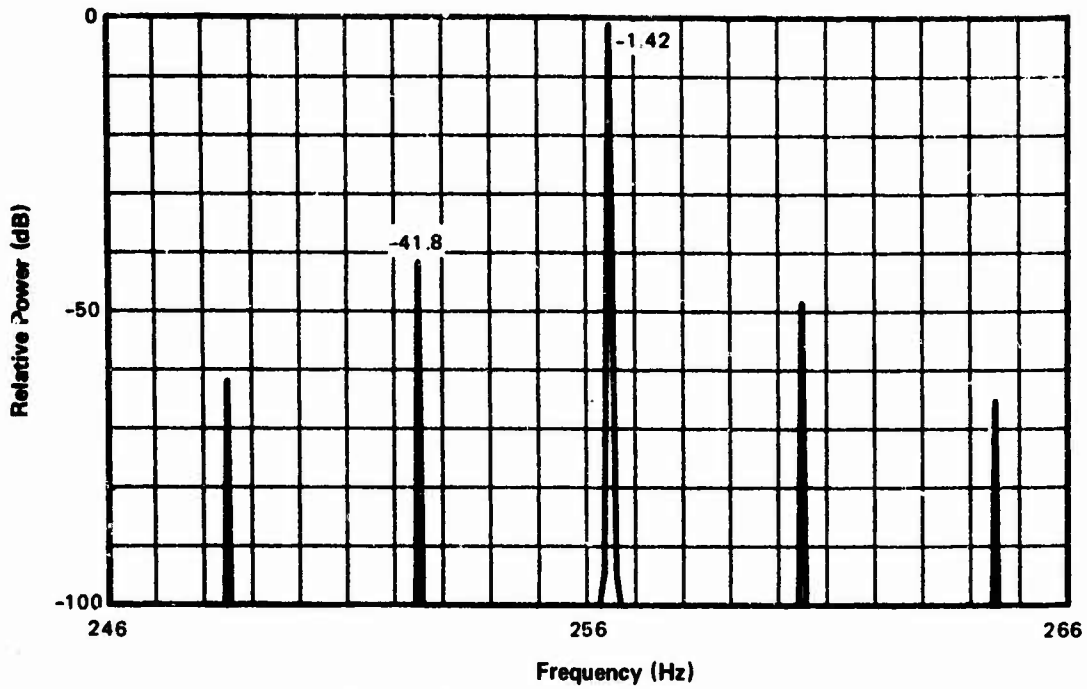

Figure 12A. f_o = 256 1/2 Hz

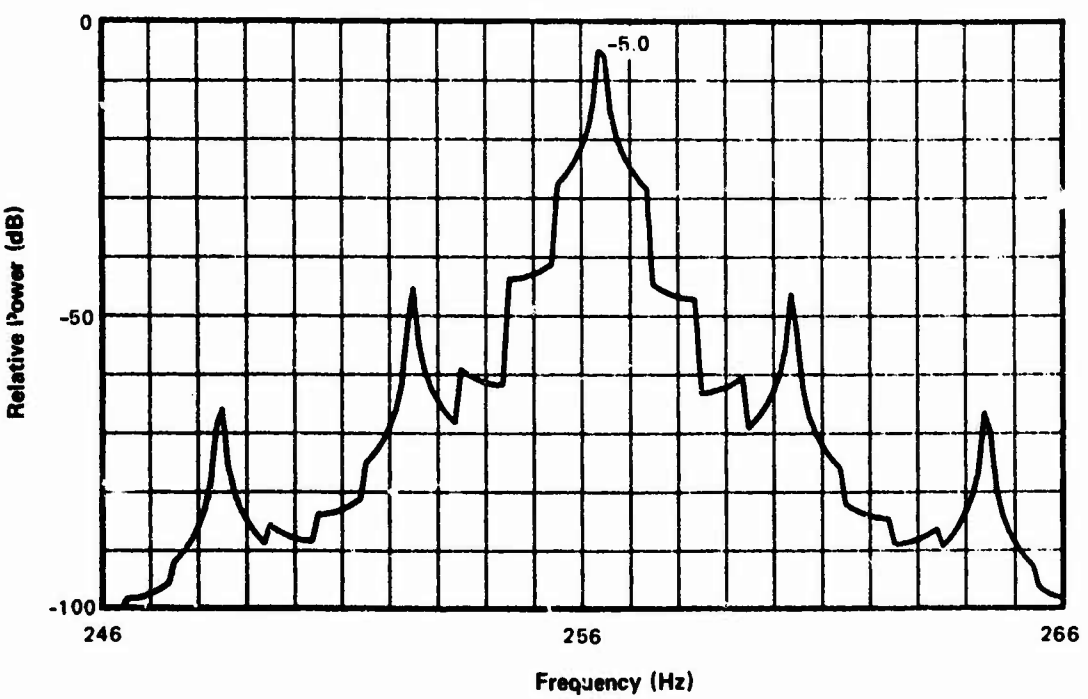

Figure 12B. f_o = 256 7/16 Hz

Figure 12. Vernier Spectrum for Flat Delay Weighting

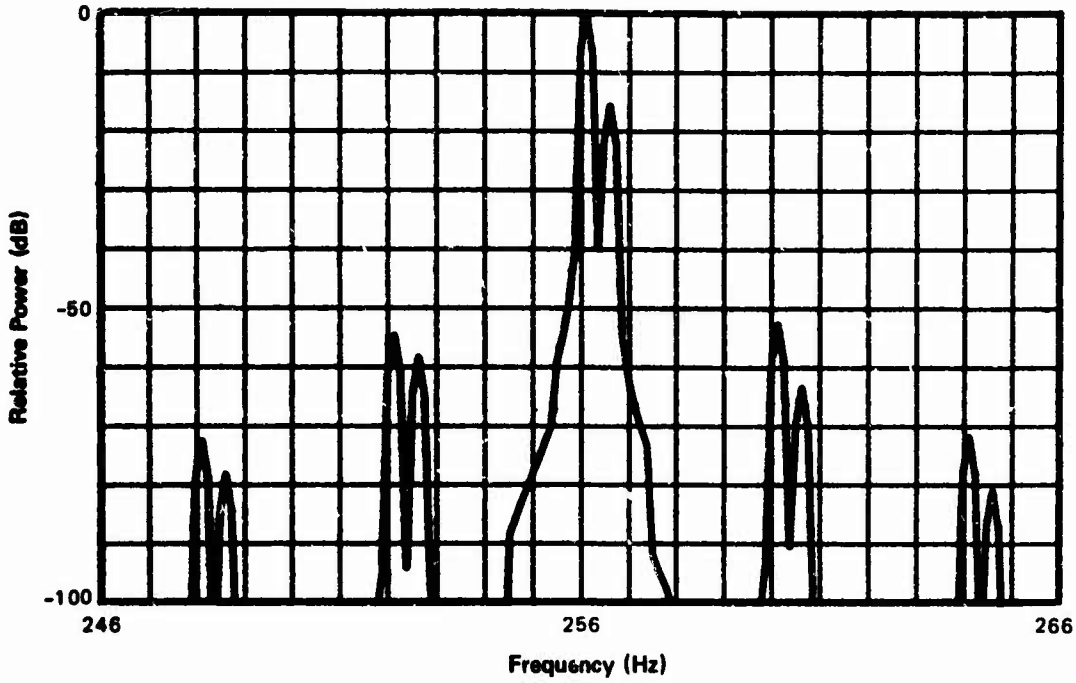

Figure 13A. f_o = 256 1/8 Hz

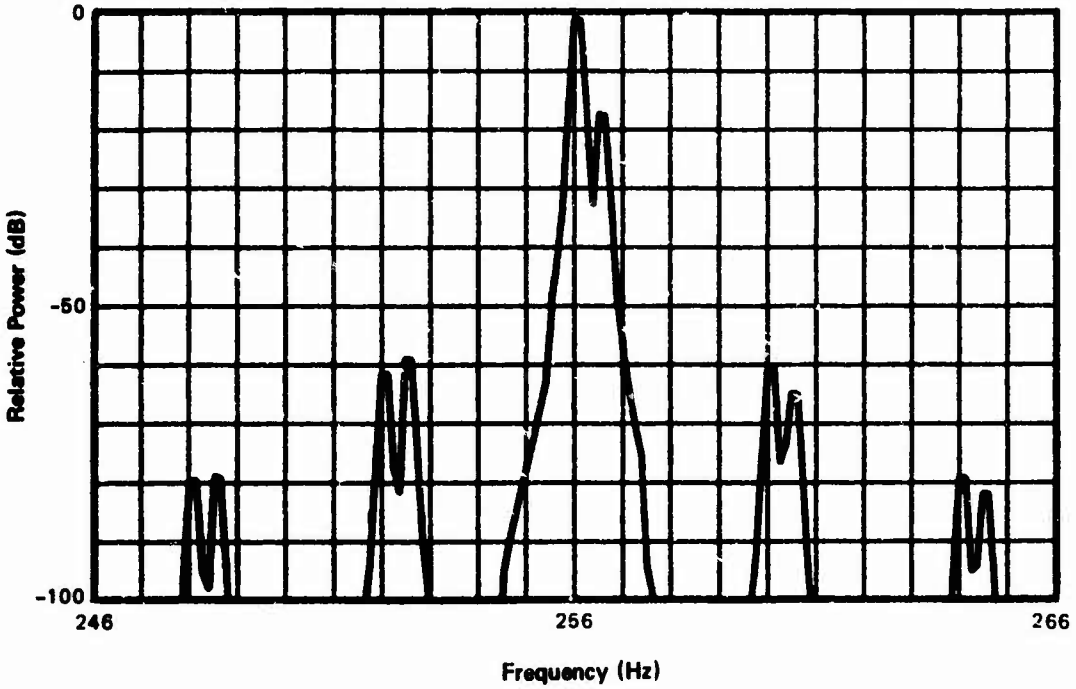

Figure 13B. f_o = 256 1/16 Hz

Figure 13. Vernier Spectrum for (Cosine)^2 Delay Weighting, Two Tones

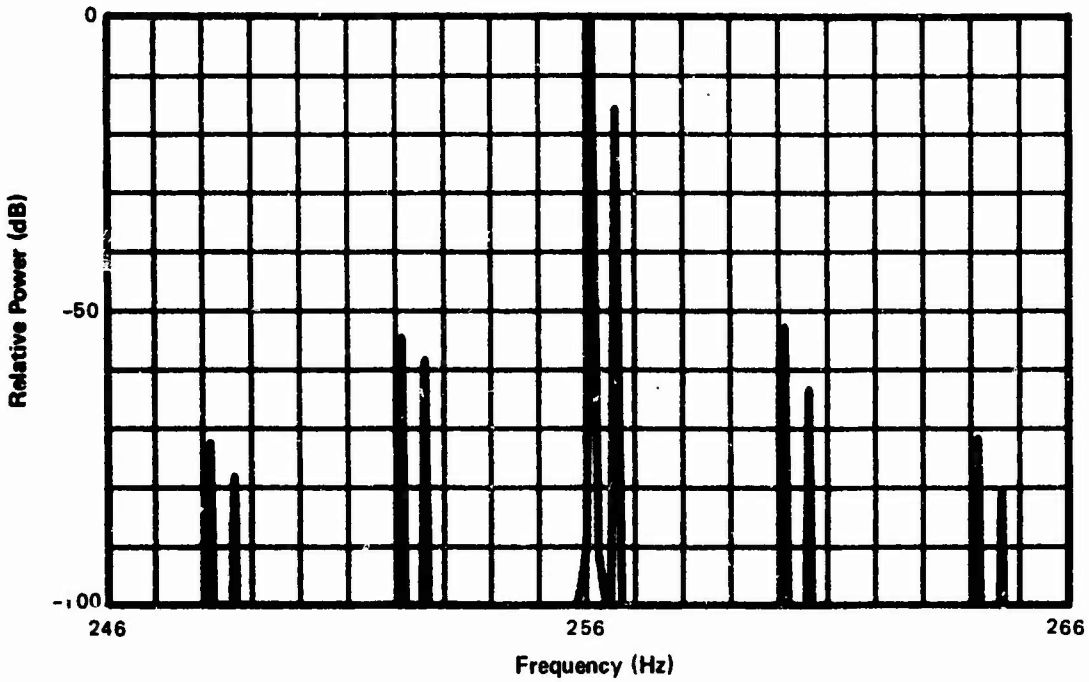

Figure 14A. f_0 = 256 1/8 Hz

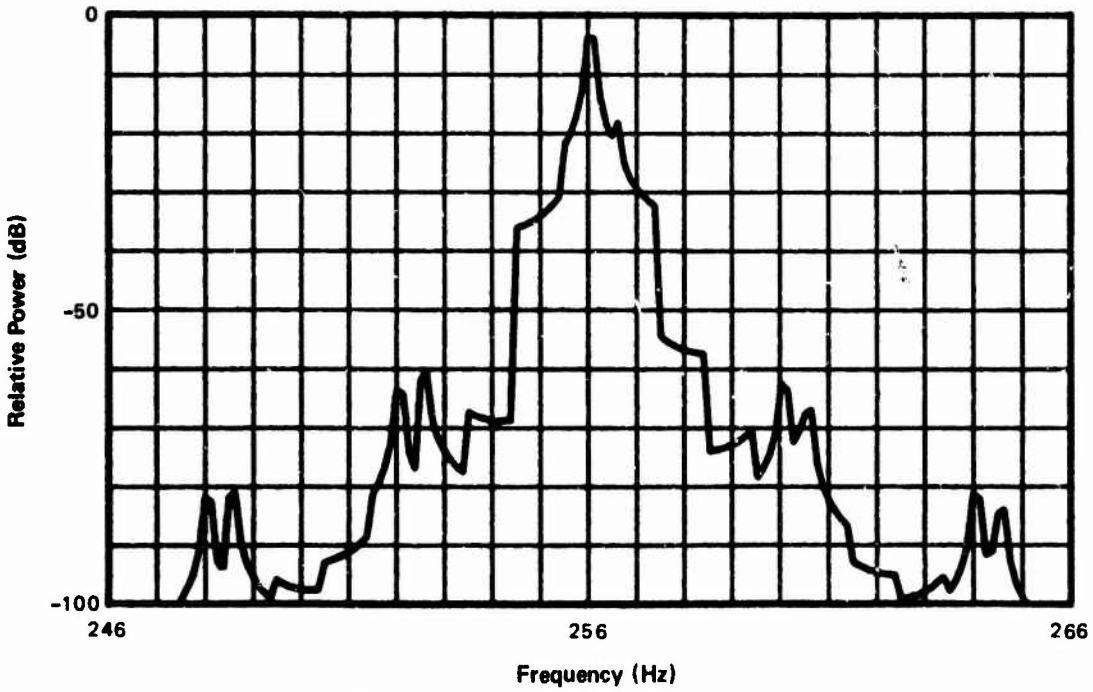

Figure 14B. f_0 = 256 1/16 Hz

Figure 14. Vernier Spectrum for Flat Delay Weighting, Two Tones

Appendix A

TWO METHODS OF COMPUTING $\sum_{n=n_o}^{n_o+N-1} \exp(-i2\pi pn/N)\, q_n$

Define

$$Q_p = \sum_{n=n_o}^{n_o+N-1} \exp(-i2\pi pn/N)\, q_n, \quad 0 \le p \le N-1 , \tag{A-1}$$

where $n_o \ge 0$. If we let $m = n - n_o$, (A-1) becomes

$$Q_p = \exp(-i2\pi pn_o/N) \sum_{m=0}^{N-1} \exp(-i2\pi pm/N)\, q_{m+n_o} . \tag{A-2}$$

The sum in (A-2) is an FFT of the sequence $\{q_n\}_{n_o}^{n_o+N-1}$.

For an alternative method, consider the general term q_n in (A-1). Then, if

$$\begin{aligned}
&\text{(a) } n = 0,\ N,\ 2N, \ldots,\ q_n \text{ gets weight } \exp(-i0) ; \\
&\text{(b) } n = 1,\ N+1,\ 2N+1, \ldots,\ q_n \text{ gets weight } \exp(-i2\pi p/N) ; \\
&\quad\vdots \\
&\text{(c) } n = N-1,\ 2N-1,\ 3N-1, \ldots,\ q_n \text{ gets weight } \exp(-i2\pi p(N-1)/N) .
\end{aligned} \tag{A-3}$$

So, if we define $\tilde{n} = n \bmod N$, then case

$$\begin{aligned}
&\text{(a) corresponds to } \tilde{n} = 0 ; \\
&\text{(b) corresponds to } \tilde{n} = 1 ; \\
&\quad\vdots \\
&\text{(c) corresponds to } \tilde{n} = N-1 .
\end{aligned} \tag{A-4}$$

Therefore, let

$$V_{\tilde{n}} = q_n , \quad n_o \le n \le n_o + N - 1 , \tag{A-5}$$

in which case

$$Q_p = \sum_{\tilde{n}=0}^{N-1} \exp(-i2\pi p\tilde{n}/N)\, v_{\tilde{n}}\ ,\ 0 \le p \le N-1\ ; \qquad \text{(A-6)}$$

this is simply an FFT of $\{v_{\tilde{n}}\}_0^{N-1}$, with no phase factor necessary. Equation (A-5) corresponds to filling up the $v_{\tilde{n}}$ array, from the given quantities q_n, starting from the nonzero position, n_0 mod N, and cycling around to position 0.

To apply these results to (10), suppose weight w is nonzero for $t > 0$. Then if n_0 is the smallest integer such that $n_0 \ge k\,S/\Delta$, (10) can be expressed as

$$a\left(\frac{p}{N\Delta},\ kS\right) = \Delta \sum_{n=n_0}^{n_0+N-1} \exp(-i2\pi pn/N)\, x(n\Delta)\, w(n\Delta - kS)\ . \qquad \text{(A-7)}$$

This is of the form of (A-1) if we identify

$$q_n = x(n\Delta)\, w(n\Delta - kS)\ . \qquad \text{(A-8)}$$

Appendix B

DERIVATION OF VERNIER SPECTRUM

From the first line of (7) in the main text, there follows immediately

$$Y(f,\nu) = A(f,\nu) \bullet D(\nu) \bullet \delta_{1/\delta}(\nu) , \tag{B-1}$$

where all convolutions are on ν, for f fixed. Then using (6), we obtain

$$\begin{aligned} A(f,\nu) &= \int d\tau \ \exp(-i2\pi\nu\tau)\ a(f,\tau) \\ &= \int d\tau \ \exp(-i2\pi\nu\tau) \int dt \exp(-i2\pi ft)\ x(t)\ w(t-\tau)\ \Delta\delta_{\Delta}(t) \\ &= W(-\nu)\int dt \exp(-i2\pi(f+\nu)\ t)\ x(t)\ \Delta\delta_{\Delta}(t) \\ &= W(-\nu) \sum_{m} X\left(f+\nu-\frac{m}{\Delta}\right) . \end{aligned} \tag{B-2}$$

Substituting (B-2) in (B-1), we have

$$Y(f,\nu) = \left[W(-\nu)\sum_{m} X\left(f+\nu-\frac{m}{\Delta}\right)\right] \bullet D(\nu) \bullet \delta_{1/\delta}(\nu) . \tag{B-3}$$

Appendix C

SAMPLE PROGRAM

The program furnished below is illustrative of the vernier technique. It has been written for

$$\Delta\,(\mathrm{DEL}) = \frac{1}{1024}\ \text{seconds},\ \mathrm{N} = 1024,\ \mathrm{M} = 32,\ \mathrm{S} = \frac{1}{4}\ \text{sec}$$
$$\mathrm{f_o(F0)} = 256(1/16)\ 256\frac{1}{2}\ , \qquad \text{(C-1)}$$

but could be easily changed to other cases. The input data are furnished by internal functions XREAL and XIMAG; currently, two tones of relative strength -15 dB and separation 1/2 Hz are incorporated. Loop 1 in the main program accomplishes Hanning temporal weighting, while loop 2 accomplishes Hanning delay weighting. The subroutines MKLFFT and QTRCOS are detailed in reference 7. The method in this program employed the cycling technique described in appendix A.

```
      PARAMETER N=1024,M=32,N4=N/4+1,M4=M/4+1
      INTEGER PS
      DIMENSION ZR(N),ZI(N),W(N),D(M),AR(21,M),AI(21,M),ADR(M),ADI(M),
     $DB(M),CN(N4),CM(M4),Z(200),X(168),Y(168)
      SQ=10.**(-.75)
      TPIM=2.*3.14159265/(M+1)
      TPIN=2.*3.14159265/N
      M1=M-1
      N1=N-1
      DEL=1./N
      IS=N/4
      S=IS*DEL
      IM=INT(LOG(FLOAT(M))*1.4427+.5)
      CALL QTRCOS(CN,N)
      CALL QTRCOS(CM,M)
      CALL MODESG(Z,0)
      CALL SUBJEG(Z,5.,-100.,165.,0.)
      CALL OBJCTG(Z,600.,1400.,2425.,2350.)
      DO 1 MS=0,N1
1     W(MS+1)=1.-COS(TPIN*MS)
      DO 2 KS=0,M1
```

```
2       D(KS+1)=1.-COS(TPIM*(KS+1))
        DO 13 IC=1,168
13      X(IC)=IC
        DO 12 IF=0,8
        F0=256.+IF*.0625
        DO 3 KS=0,M1
        N0=IS*KS
        NU=N0+N1
        DO 4 NS=N0,NU
        NT=MOD(NS,N)
        ZR(NT+1)=XREAL(NS*DEL)*W(NS-N0+1)
        ZI(NT+1)=XIMAG(NS*DEL)*W(NS-N0+1)
4       CONTINUE
        CALL MKLFFT(ZR,ZI,CN,10,-1)
        DO 5 PS=246,266
        AR(PS-245,KS+1)= DEL*ZR(PS+1)
        AI(PS-245,KS+1)= DEL*ZI(PS+1)
5       CONTINUE
3       CONTINUE
        DO 6 PS=246,266
        DO 7 KS=0,M1
        ADR(KS+1)=S*AR(PS-245,KS+1)*D(KS+1)
        ADI(KS+1)=S*AI(PS-245,KS+1)*D(KS+1)
7       CONTINUE
        CALL MKLFFT(ADR,ADI,CM,IM,-1)
        IF(IF.EQ.0.AND.PS.EQ.256) PEAK=10.*LOG10(ADR(1)**2+ADI(1)**2)
        DO 8 KS=0,M1
        AR(PS-245,KS+1)=ADR(KS+1)
        AI(PS-245,KS+1)=ADI(KS+1)
8       CONTINUE
6       CONTINUE
        DO 9 PS=246,266
        IC=(PS-246)*8
        DO 10 MS=0,M1
        A=AR(PS-245,MS+1)**2+AI(PS-245,MS+1)**2
        A=MAX(A,1.E-36)
        DB(MS+1)=10.*LOG10(A)-PEAK
10      CONTINUE
        PRINT 14, PS
14      FORMAT(///I10/)
        PRINT 11, DB
11      FORMAT(/6E15.6)
        Y(IC+1)=DB(M-3)
        Y(IC+2)=DB(M-2)
        Y(IC+3)=DB(M-1)
        Y(IC+4)=DB(M)
        Y(IC+5)=DB(1)
        Y(IC+6)=DB(2)
        Y(IC+7)=DB(3)
        Y(IC+8)=DB(4)
9       CONTINUE
        SIDE=-200.
        DO 17 IC=1,168
        IF(IC.GE.69.AND.IC.LE.109) GO TO 17
        SIDE=MAX(SIDE,Y(IC))
```

```
17    CONTINUE
      PRINT 18, SIDE
18    FORMAT(/' PEAK SIDELOBE IS',E14.8)
      CALL SETSMG(Z,30,1.)
      DO 15 IP=10,90,10
      CALL LINESG(Z,0.  5.,-FLOAT(IP))
15    CALL LINESG(Z,1.165.,-FLOAT(IP))
      DO 16 IP=13,157.8
      CALL LINESG(Z,0.FLOAT(IP),0.)
16    CALL LINESG(Z,1.FLOAT(IP),-100.)
      CALL SETSMG(Z,30,2.)
      CALL LINESG(Z,0.5.,-100.)
      CALL LINESG(Z,1.5.,0.)
      CALL LINESG(Z,1.165.,0.)
      CALL LINESG(Z,1.165.,-100.)
      CALL LINESG(Z,1.5.,-100.)
      CALL LINESG(Z,168,X,Y)
      CALL PAGEG(Z,0,3,1)
12    CONTINUE
      CALL EXITG(Z)
      PRINT 11, PEAK
      FUNCTION XREAL(T)
      XREAL=COS(2.*3.141592654*F0*T)
     $     +COS(2.*3.141592654*(F0+.5)*T)*S0
      RETURN
      FUNCTION XIMAG(T)
      XIMAG=SIN(2.*3.141592654*F0*T)
     $     +SIN(2.*3.141592654*(F0+.5)*T)*S0
      RETURN
      END
```

Appendix D

EFFECT OF (COSINE)^n TIME WEIGHTING

Let us define the spectrum of unweighted data x as

$$Z(f) \equiv \int dt \exp(-i2\pi ft)\, x(t)\, \Delta\delta_\Delta(t) = \Delta \sum_{k=0}^{N-1} \exp(-i2\pi k\Delta f)\, x(k\Delta), \quad \text{(D-1)}$$

and that corresponding to weighting w as

$$\begin{aligned} Z_w(f) &\equiv \int dt \exp(-i2\pi ft)\, x(t)\, w(t)\, \Delta\delta_\Delta(t) = Z(f) \bullet W(f) \\ &= \Delta \sum_{k=0}^{N-1} \exp(-i2\pi k\Delta f)\, x(k\Delta)\, w(k\Delta) \ . \end{aligned} \quad \text{(D-2)}$$

Now for (cosine)^n time weighting, we have*

$$w(k\Delta) = \sin^n(k\pi/N), \quad 0 \le k \le N-1 \ . \quad \text{(D-3)}$$

Substituting (D-3) in (D-2), there follows

$$\begin{aligned} Z_w(f) &= \Delta \sum_{k=0}^{N-1} \exp(-i2\pi k\Delta f)\, x(k\Delta) \left(\frac{1}{i2}\right)^n \left[\exp(ik\pi/N) - \exp(-ik\pi/N)\right]^n \\ &= \Delta \sum_{k=0}^{N-1} \exp(-i2\pi k\Delta f)\, x(k\Delta) \left(\frac{1}{i2}\right)^n \sum_{j=0}^{n} (-1)^j \binom{n}{j} \exp\left[i\frac{k\pi}{N}(n-2j)\right] \\ &= \Delta\left(\frac{1}{i2}\right)^n \sum_{j=0}^{n} (-1)^j \binom{n}{j} \sum_{k=0}^{N-1} x(k\Delta) \exp\left[-i2\pi k\Delta\left(f - \frac{n-2j}{2N\Delta}\right)\right] \\ &= \left(\frac{1}{i2}\right)^n \sum_{j=0}^{n} (-1)^j \binom{n}{j} Z\left(f - \frac{n-2j}{2N\Delta}\right) \ , \end{aligned} \quad \text{(D-4)}$$

the last step via use of (D-1). This result yields (20).

*See the first footnote to equation (19) of the main text for the explanation of $\sin^n$ in (D-3).

For the special case of $n = 1$, (D-4) becomes

$$Z_W(f) = i\,1/2\left[Z\left(f - \frac{1}{2N\Delta}\right) - Z\left(f + \frac{1}{2N\Delta}\right)\right], \qquad \text{(D-5)}$$

and in particular,

$$Z_W\left(\frac{n}{N\Delta} + \frac{1}{2N\Delta}\right) = i\,1/2\left[Z\left(\frac{n}{N\Delta}\right) - Z\left(\frac{n+1}{N\Delta}\right)\right]. \qquad \text{(D-6)}$$

The right-hand side of (D-6) involves two adjacent spectral values as afforded by the standard N-point FFT in (D-1). The left-hand side of (D-6) is the spectral value of Z_W at the frequency halfway between the above two spectral locations. Thus, under this interpretation of the right-hand side of (D-6), the desirable sidelobe control predicted by the convolution in (D-2) can be attained. A similar interpretation is possible for (D-4) for general n.

REFERENCES

1. A. H. Nuttall, "Two Methods of Performing a Large-Size FFT by Means of Several Smaller FFTs," NUSC Technical Memorandum TC-185-72, 6 October 1972.

2. J. F. Ferrie, C. W. Nawrocki, and G. Clifford Carter, "Implementation and Results of the Modified Chirp Z-Transform," NUSC Technical Memorandum TC-191-72, 18 October 1972.

3. C. W. Nawrocki and J. F. Ferrie, "Zoom FFT — An Approximate Vernier Frequency Algorithm," NUSC Technical Memorandum SA2201-584-72, 22 November 1972.

4. G. D. Bergland, "A Guided Tour of the Fast Fourier Transform," IEEE Spectrum, vol. 6, July 1969, pp. 41-52.

5. C. L. Dolph, "A Current Distribution for Broadside Arrays Which Optimizes the Relationship Between Beam Width and Side-Lobe Level," Proceedings of the I. R. E. and Waves and Electrons, vol. 34, June 1946, pp. 335-348.

6. A. H. Nuttall, "Generation of Dolph-Chebyshev Weights for Large Numbers of Elements via a Fast Fourier Transform," NUSC Technical Memorandum TC-5-74, 15 April 1974.

7. J. F. Ferrie, G. C. Carter, and C. W. Nawrocki, "Availability of Markel's FFT Pruning Algorithm," NUSC Technical Memorandum TC-1-73, 15 January 1973.